

lightsource.ca

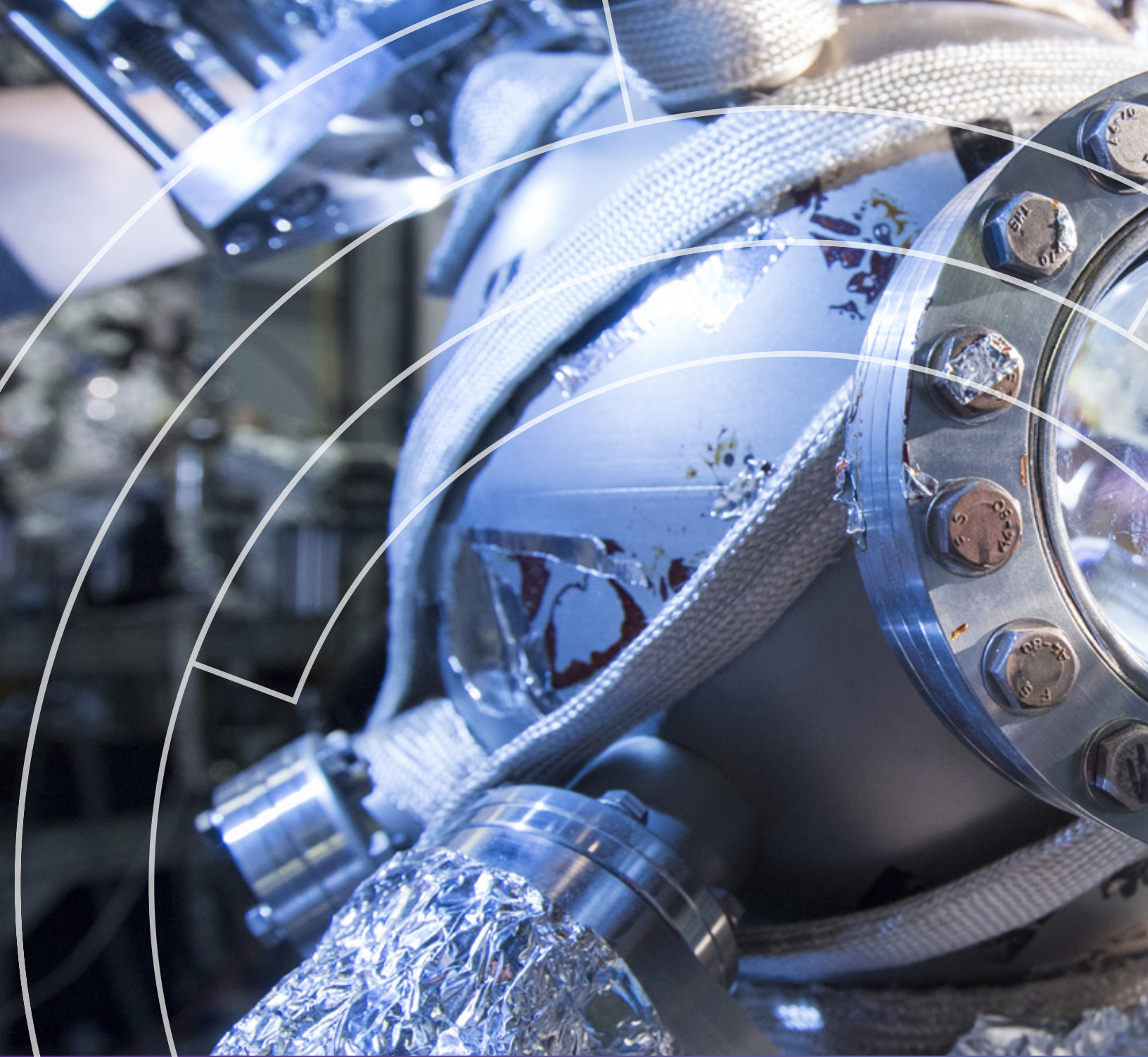
RESEARCH **REPORT** 2017



Canadian
Light
Source

Centre canadien
de rayonnement
synchrotron

THE BRIGHTEST LIGHT IN CANADA



Canadian Light Source Research Report 2017
Editor: Victoria Martinez
ISBN 978-0-9783761-8-5

© 2017 Canadian Light Source Inc. All rights reserved.

Canadian Light Source, Inc.
44 Innovation Boulevard
Saskatoon, SK, Canada S7N 2V3
Telephone: (306) 657-3500
Fax: (306) 657-3535
Email: cls@lightsource.ca

www.lightsource.ca

Layout and cover design: Reach Communications

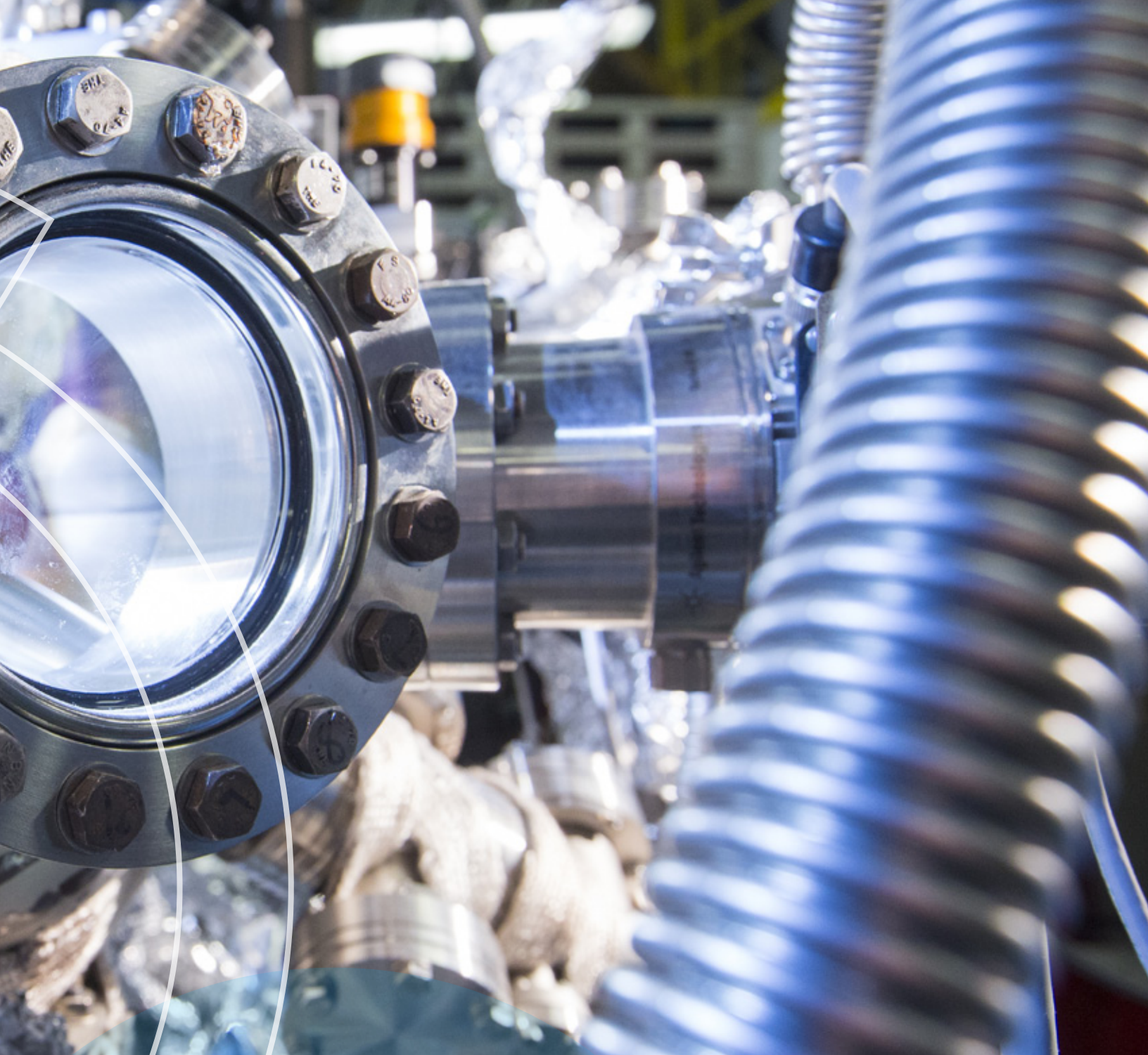






TABLE OF CONTENTS

ACKNOWLEDGEMENTS	2	FACTS AND FIGURES	30
MESSAGE FROM THE CEO	3	PHASE THREE BEAMLINE UPDATES	
YEAR IN REVIEW	4	BROCKHOUSE SECTOR.	33
2017 SCIENCE HIGHLIGHTS.	8	BIOXAS.	34
 HEALTH	10	QMSC.	35
 AGRICULTURE	15	INNOVATIONS	36
 ENVIRONMENT	20	EDUCATION PROGRAMS.	38
 ADVANCED MATERIALS	25	ACRONYM GLOSSARY.	40

ACKNOWLEDGEMENTS

FUNDING PARTNERS

The Canadian Light Source thanks all of our funding partners for their commitment to the advancement of science and innovation.

OPERATING



CAPITAL



CANADIAN USER UNIVERSITIES



MESSAGE FROM THE CEO

GETTING OUT MORE

2017 has been a year of enormous progress towards the four strategic goals of the Canadian Light Source for the coming years.

Increase impact by being a solution provider

We launched a new proposal submission portal which streamlines user processing and facility usage tracking. Importantly, it also makes it easier to use multiple beamlines within a single experiment. This is an important element in our new Solution Provider service and access model. Thanks to additional support from the Canada Foundation for Innovation, we constructed new soundproof hutches adjacent to beamlines to enhance the user experience and increase beamline productivity by improving the physical working environment.

A restructuring of user representation processes has resulted in a new, stronger user body, the Users' Executive Committee, which will increase dialogue with our most important stakeholder group and lead the community consultation process for the future of science for Canadian users of light sources.

With 90 per cent of Phase III beamlines in commissioning or fully commissioned, Phase IV beamline improvements have moved up the priority list, with the first stage of the protein crystallography (CMCF-ID) upgrade completed.

Focus research and industry sector activities in areas with greatest potential

In addition to the materials, environment and health research focus areas, agriculture has seen a major thrust. The growth in industrial projects and research in plant innovation, is a feature of this report. New insights for improved crop and plant development, fertilizers, drought and temperature resistance, and soil management are just the beginning of this major initiative.

The macromolecular crystallography program remains the leader in industrial usage and revenue, with entries to the Protein Data Bank (PDB)—critical contributions to biological and pharmaceutical research—having reached the 1,000 mark. The addition of a faster sample-changing robot is already increasing usage in this sector.

Advanced materials research in composites related to aerospace, automotive, and batteries, also continues to grow, as the search for lighter materials and greener sources of energy intensifies around the world.

In environmental science CLS continues to enable advancements in mine remediation techniques, heavy oil extraction, high efficiency catalysts to turn CO₂ into plastics, renewable resources, and energy storage, as well as remediation of contaminated groundwater and heavy metal contamination in soil and water.

Enhance and capitalize on machine science and engineering expertise

CLS welcomed Dr. Mark Boland as the new Machine Director. Mark will provide strategic leadership in the development and operation of the CLS, and in his first few months has already made great strides in engaging the broader accelerator community to begin envisioning the future.

The Canadian Nuclear Safety Commission (CNSC) approved a change in the CLS operating license to permit top up operations. Starting in May 2018, the ring will take a first major step, with no more dark periods during regular user operations. Upgrades to beamlines will continue to take advantage of the resulting constant brightness conditions.

Establish broad awareness of the CLS as an accessible driver of innovation

The CLS's focus is to continue building and strengthening ties with stakeholders at the local, provincial, national and international levels. Through our vigorous outreach and educational programs, creative social and traditional media efforts, and increased staff engagement in the local community, we ensure increased awareness about CLS science. Nationally, our scientists are working with researchers from over 50 Canadian universities, presenting at conferences, and encouraging new light source users to consider CLS in their research programs.

Internationally, the CLS is also more engaged than ever. Through a new collaboration agreement with Max-IV in Sweden, the first next generation light source in the world, and personnel exchanges with the largest synchrotron facility, Spring-8, we are ensuring that CLS staff have access to the most advanced accelerator technologies and experts. CLS represents the Government of Canada as council observers on the development of the Middle East synchrotron in Jordan, SESAME, created under the auspices of UNESCO. Last, but not least, the CLS is an active partner in the Lightsources for Africa, the Americas, Asia and Middle East Project (LAAAMP), a joint program of the IUPAC and the IUCr with a mandate to enhance advanced light source and crystallographic sciences in developing countries.

It is thanks to the continued support of our funding partners, the Canada Foundation for Innovation, Natural Sciences and Engineering Research Council, National Research Council of Canada, Canadian Institutes of Health Research, the Government of Saskatchewan and the University of Saskatchewan that we ensure the over 1,000 researchers who use CLS per year achieve their scientific goals: On behalf of all of us at CLS and the entire light source scientific community, thank you.

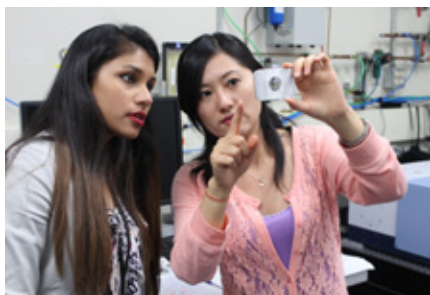
Robert Lamb
CEO



YEAR IN REVIEW

JANUARY

CLS awarded \$48 million to advance innovation: Canada's Science Minister Kirsty Duncan announced on Jan. 9 that \$328 million would be invested through the Major Science Initiatives fund of the Canada Foundation for Innovation to support operations at 17 national science centres over the next three to five years. The CLS was one of three University of Saskatchewan facilities to receive funding.

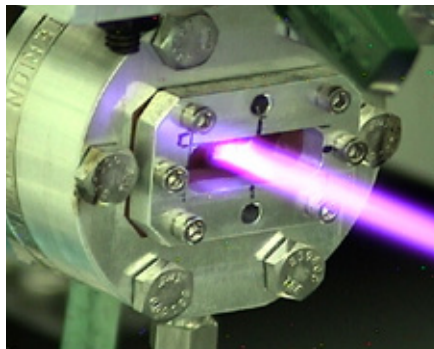


Science minister visits CLS: We were thrilled to host the federal minister of science, the Honourable Kirsty Duncan, on Jan. 18. We showed her the amazing work our scientists are doing in health, agriculture, environment, climate change, and advanced materials. We also hosted a round table discussion on innovation in our province and Canada.



Monochromatic undulator beam in the BioXAS imaging endstation: One of our newest beamlines, BioXAS, saw first light in January. Once completed, BioXAS will be

tailored for health and biological studies of metals in living systems.



FEBRUARY

MOU with MAX IV Laboratory: CLS CEO Robert Lamb signed a memorandum of understanding with MAX IV Laboratory in Lund, Sweden, on Feb. 22. The two research facilities will collaborate closely in a partnership that will continue to advance science and innovation in Canada.



MARCH

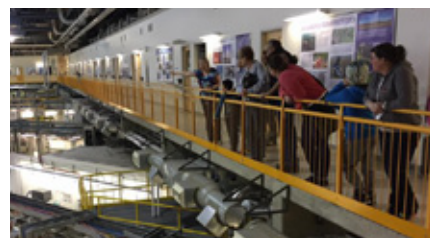
HXMA wiggler upgrade: A major upgrade to the HXMA wiggler was installed during the 2017 spring shutdown. This upgrade included a replacement of the entire cryogenic system and associated components with major changes at the current lead blocks, cold figures and wiggler safety path. The wiggler magnetic field is increased from the 1.9 tesla designed value to 2.2 tesla as a result of the highly efficient new cryo-system and components. The HXMA beamline's availability and

reliability has significantly improved since the upgrade.



Innovation150 celebrations begin:

Innovation 150, a nationwide program from five leading science organizations, celebrated Canada's innovative past and the ideas and ingenuity that will propel our future. The interactive, yearlong program offered awe inspiring experiences in science, technology, and innovation across the country for Canada's 150th anniversary. Celebrations in Saskatchewan launched with dedicated after-hours CLS evening tours for hundreds of members of the public.



APRIL

Science Odyssey: Sponsored by the Natural Sciences and Engineering Research Council of Canada (NSERC), Science Odyssey is Canada's largest annual celebration of science, technology, engineering and mathematics. CLS hosted several hundred members of the public during this annual science outreach event.





Light and colour entertains air travelers of all ages: The CLS, the Children's Discovery Museum of Saskatchewan, and the Saskatoon Airport Authority launched *Innovation for All Ages*, a fun "lite brite" interactive display in the departures area at the Saskatoon International Airport. The display aims to educate children and their parents about how light in all its forms and colours is essential for science, and how it has been used for some of the most exciting scientific discoveries in the world.



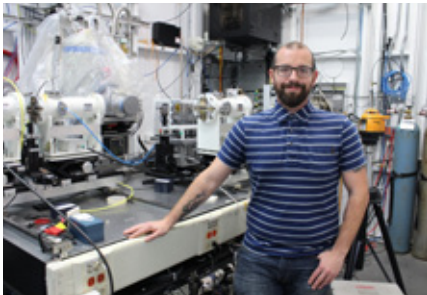
MAY

Annual award recipients announced: Congratulations to the winners of this year's awards.

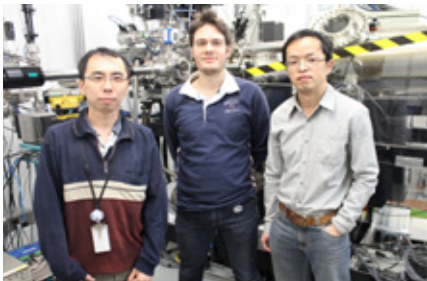
• **Allen Pratt Award**
T.K. Sham, Department of Chemistry, Western University. The Allen Pratt Award recognizes outstanding service and dedication to the CLS and the Canadian synchrotron community by a current user who has or team of users that has made a significant recent contribution.



• **User Support Award**
Peter Blanchard, VESPERs. The User Support Award is given to a CLS staff member who has provided outstanding help to visiting researchers.



• **Young Investigator Award**
Riccardo Comin, Department of Physics, Massachusetts Institute of Technology. The Young Investigator Excellence Award is given to an individual who is an early-career researcher with an excellent publication and/or technical contribution in which the CLS has played a substantial role.

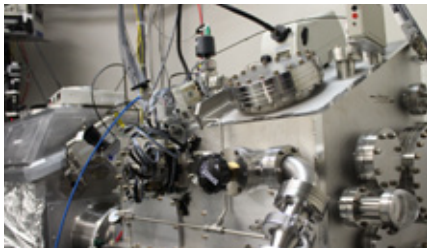


Open SESAME - CLS and synchrotron in Middle East develop strong ties:
The Synchrotron-light for Experimental Science and Applications in the Middle East (SESAME) facility, located in Jordan, officially opened on May 16. Our CEO Robert Lamb is one of two Canadian representatives on the SESAME Council as Canada has observer status. Observer status opens the door for joint research initiatives for faculty and graduate students, exchanges, and training opportunities, including having SESAME

researchers participate in CLS workshops and summer schools.

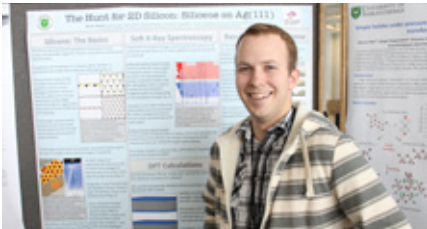


New SM Cryo-STXM: The Cryo-STXM endstation's operation was demonstrated to one of the SM beamline's key funders, Automotive Fuel Cell Cooperation, and the first complete CT dataset below -180°C was acquired shortly after the demonstration. This was a key milestone of the SM Cryo-STXM technical commissioning.



JUNE

G. Michael Bancroft PhD Thesis award winner announced: Neil Johnson, PhD U of S. The Bancroft award is awarded based on the quality of the scientific research within the context of the field, the importance of synchrotron radiation from the CLS for answering the scientific questions posed, and the quality and capability of the candidate based on their CV and the letter of recommendation.



YEAR IN REVIEW

MX Data Collection School: At this five day hands-on synchrotron data collection school, 20 researchers from across Canada learned to use the CMCF beamlines remotely as well as on-site. This session had a special focus on structure solution with Dr. Jeffrey Lee from the University of Toronto. Since 2010, the school has been integral to training over 160 crystallographers.



JULY

The CLS Summer School: This annual program offered students, faculty, and industry scientists interested in becoming CLS users hands-on, practical experience with various synchrotron techniques, as well as sample preparation, data collection and analysis, proposal writing, and case studies.



Staff Canada 150 celebration: The entire staff dressed in red and white to celebrate Canada's 150th birthday. In recognition of

our, and Canada's, cultural diversity, staff also celebrated their countries of heritage with flags.



AUGUST

Teachers' Workshop: This professional development opportunity focused on experiential learning and inquiry-based pedagogy. CLS opened its doors to educators from across Canada for a unique learning opportunity in August. Teachers participated in experiments, networked with researchers, explored the facility, and connected with current research.



SEPTEMBER

Mark Boland joins CLS as new machine director: Mark Boland began his dual role as the machine director for the CLS and associate professor in the Department of Physics and Engineering Physics at the U of S. As machine director, he provides

strategic leadership in the development and operation of the CLS.



Nuit Blanche 2017: CLS was proud to be a part of Saskatoon's Nuit Blanche nighttime arts festival. Artist JS Gauthier presented *Within Measure*, an original series of digital art works created using cutting-edge 3D synchrotron imaging techniques in collaboration with Brian Eames, the U of S, and the CLS.



OCTOBER

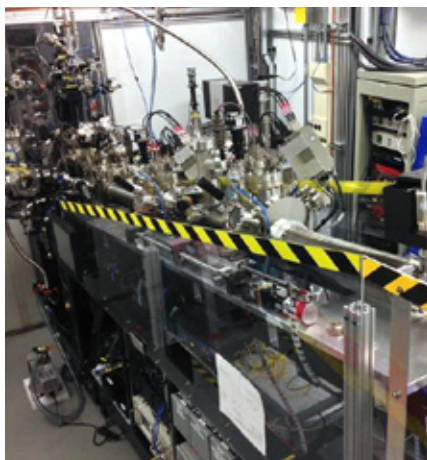
AIMday Imaging: On Oct. 18, Saskatchewan academic researchers and industry representatives from various sectors met at a U of S-led event to discuss global challenges in the agriculture, healthcare, and resource sectors. CLS

scientists were matched with industry partners to collaborate on specific projects.



Successful REIXS spectrometer repair:

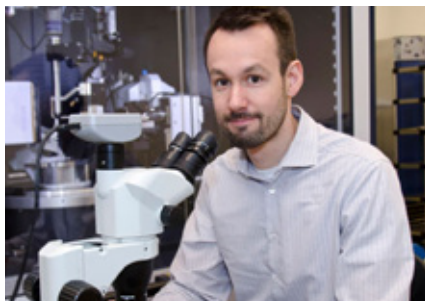
The RIXS endstation at the REIXS beamline required a major upgrade and repair so that components that need regular service would be outside the endstation's vacuum chamber. This project was completed on an ambitious timeline, and the endstation now provides two detectors providing two ranges: 525-1125 nm and 1425-2125 nm.



NOVEMBER

Crystallographers identify 1,000 protein structures:

Scientists have solved 1,000 protein structures using data collected at the CMCF beamlines. These have been added to the Protein Data Bank – a global collection of structures solved by researchers globally. Researchers have also published 500 scientific papers based on work using our crystallography beamlines.



BMIT gets new heat-removal filter:

The filter, designed to withstand the power of the BMIT wiggler beam, was installed in the beamline's front end. The assembly is composed of a large synthetic diamond disk and specifically designed heat sink. It removes up to 2.5 kW of heat from the X-ray beam and provides the necessary protection for other X-ray optical elements installed in the beamline. With the addition of the diamond filter, reliability of the beamline is considerably improved.



DECEMBER

First data with new CMCF-ID sample changer:

The newly-installed IRELEC ISARA sample changer on CMCF-ID reduces sample change times from over two minutes to under 30 seconds allowing for a much higher samples throughput.



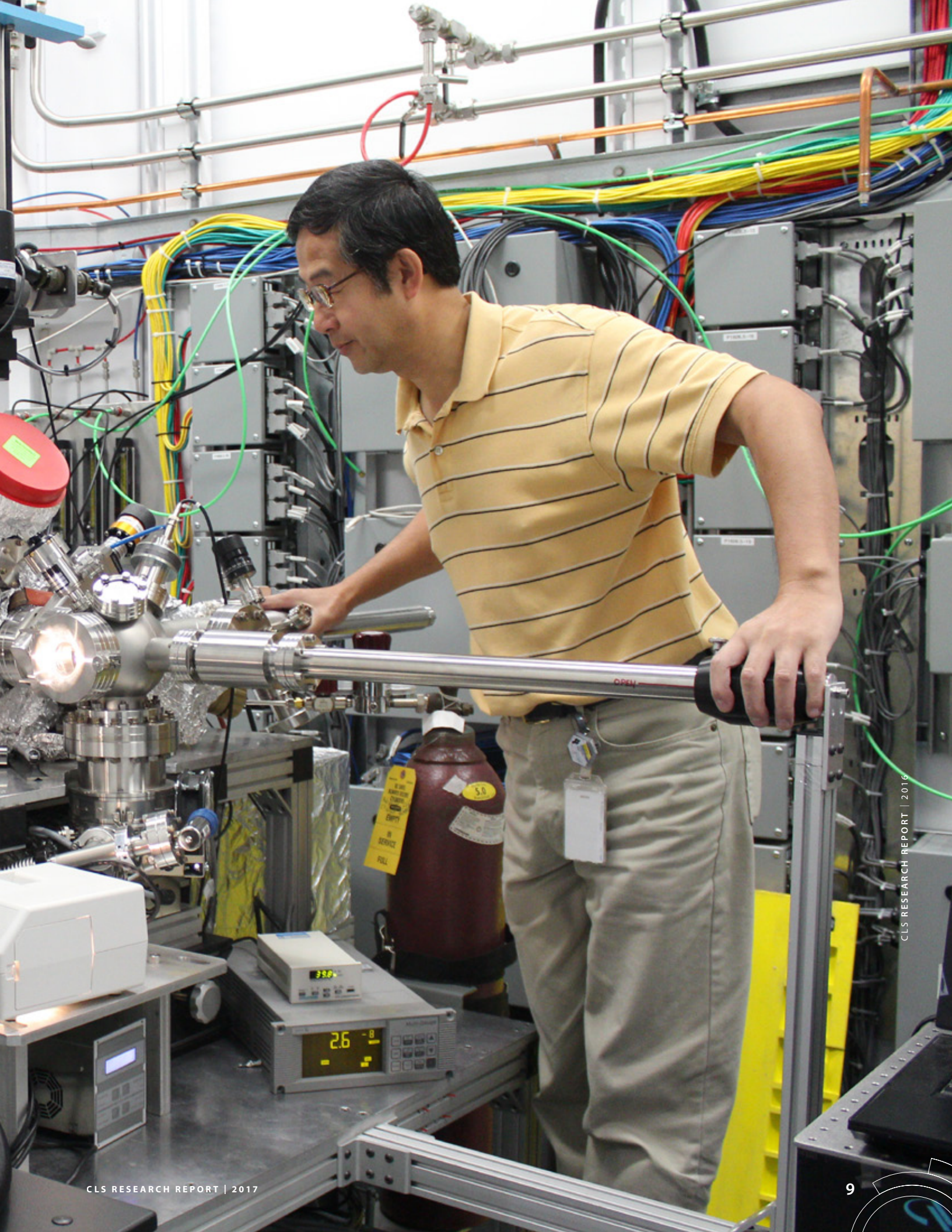
CMCF data collection interface updated:

Mx Data Collector (MxDC), was updated with new features, including improved automation options. The sample management interface, Mx Laboratory Information Virtual Environment (MxLIVE) received an update, streamlining sample management and adding new data management and download options.





SCIENCE HIGHLIGHTS



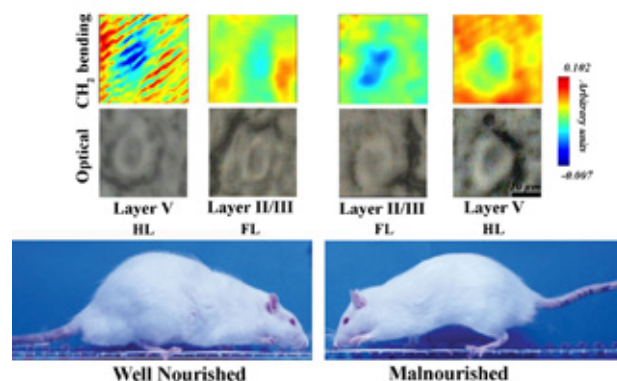


HEALTH

Parallel changes in cortical neuron biochemistry and motor function in protein-energy malnourished adult rats

Mid-IR

A lack of adequate nutrients, whether due to diet or illnesses such as stroke, may cause protein-energy malnutrition (PEM), with harmful effects on the brain. This research sought to identify effects of PEM in adult brain that could underlie abnormal skilled motor function. The biochemical signature of brain cells at the cellular and subcellular levels by FTIR spectroscopy, using a synchrotron generated light source, showed that mature cortical neurons were vulnerable to PEM. The researchers suggest this may be one mechanism by which PEM exacerbates the detrimental effects of stroke, making PEM itself an important therapeutic target.



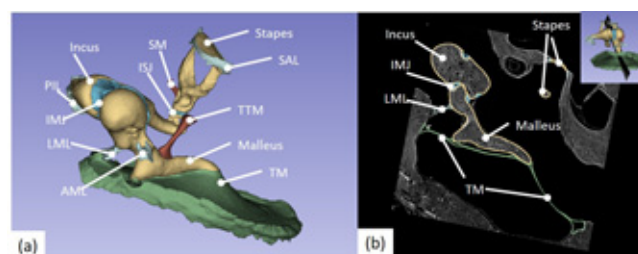
Representative false-color images of neurons from forelimb (FL) and hindlimb (HL) regions of the motor cortex underneath the $\delta(\text{CH}_2)$ band ($1475\text{--}1462\text{ cm}^{-1}$) by FTIR spectroscopy using a synchrotron light source generated at the CLS. Representative adult rats are being tested for their walking ability on the horizontal ladder. Note the abnormal biochemical and behavioral patterns in the protein-energy malnourished rat.

Alaverdashvili, Mariam, Mark J. Hackett, Sally Caine, and Phyllis G. Paterson. "Parallel changes in cortical neuron biochemistry and motor function in protein-energy malnourished adult rats." *NeuroImage* 149 (2017): 275-284.

Improved middle ear soft-tissue visualization using synchrotron radiation phase-contrast imaging

BMIT

High resolution images of structures are vital to building computational models of the ear, which in turn help investigators understand the relationship between structure and function. There are several challenges to getting good images of the middle ear, which is made up of three mm-scale bones, connected by ligaments, muscles, and nerves. In order to develop prostheses and implants, detailed information about both the hard and soft tissue is invaluable. Synchrotron PCI makes it possible to image both in three dimensions with a high degree of accuracy without extensive sample preparation, as shown in this paper.



Computer model generated from PCI of the human middle ear.

a) 3D model with tympanic membrane (TM), middle ear ossicles (malleus, incus and stapes) and soft tissue structures [tensor tympani muscle (TTM), incudostapedial joint (ISJ), stapedial annular ligament (SAL), stapedius muscle (SM), posterior incudal ligament (PIL), incudomalleolar joint (IMJ), lateral malleolar ligament (LML) and anterior malleolar ligament (AML)].

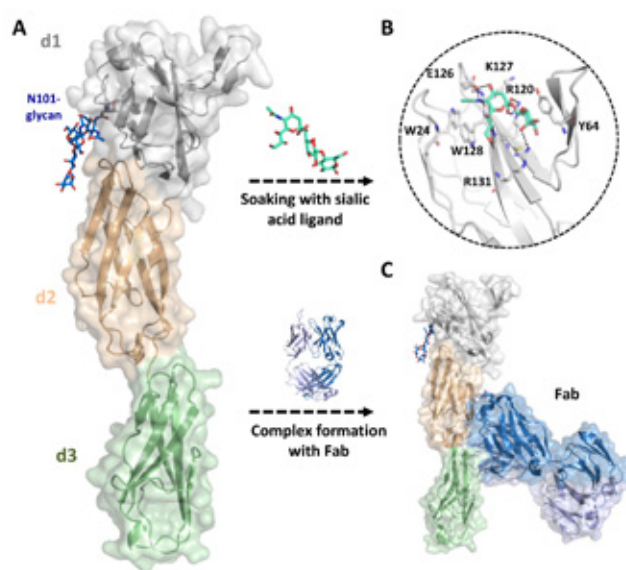
b) Image plane illustrating the sharpness of the soft-tissue boundaries and the adjacent bones. The spatial location of this plane is given in the top right corner.

Elfarnawany, Mai, Seyed Alireza Rohani, Soroush Ghomashchi, Daniel G. Allen, Ning Zhu, Sumit K. Agrawal, and Hanif M. Ladak. "Improved middle-ear soft-tissue visualization using synchrotron radiation phase-contrast imaging." *Hearing Research* 354 (2017): 1-8.

Molecular basis of human CD22 function and therapeutic targeting

CMCF

CD22 is a B cell surface protein involved in regulating the immune response, which when dysregulated can cause blood cancers and autoimmune diseases such as Type 1 diabetes and arthritis. CD22's importance to the immune response has been known for some time, but a detailed molecular understanding has been lacking. This research presents a detailed structural model of this key immune component. Combining X-ray crystallography, SAXS and electron microscopy, the researchers describe the molecular structure of human CD22 alone, as well as in complex with a sialyllactose ligand and a therapeutic antibody.



Three-dimensional structure of human CD22 extracellular domain.

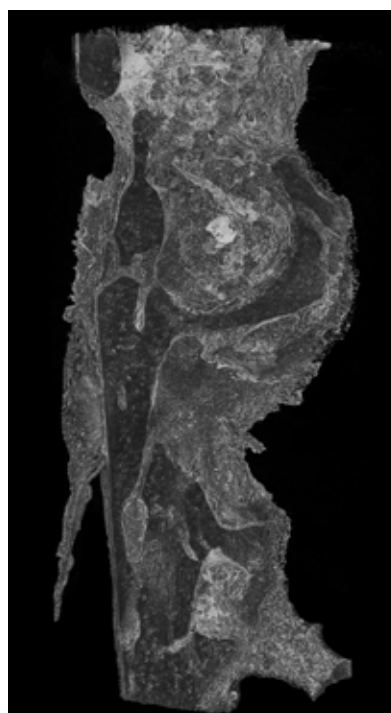
- a) Crystal structure of the three N-terminal Ig domains of human CD22 (d1–d3).
- b) Zoom view of the α2-6 sialyllactose ligand bound to human CD22 d1 domain (gray).
- c) Antigenic surface of CD22 d1-d3 recognized by therapeutic antibody epratuzumab.

Ereño-Orbea, June, Taylor Sicard, Hong Cui, Mohammad T. Mazhab-Jafari, Samir Benlekbir, Alba Guarné, John L. Rubinstein, and Jean-Philippe Julien. "Molecular basis of human CD22 function and therapeutic targeting." *Nature communications* 8, no. 1 (2017): 764.

Evaluating differential nuclear DNA yield rates and osteocyte numbers among human bone tissue types: A synchrotron radiation micro-CT approach

BMIT

Sampling DNA from bone is an important forensic tool. Smaller bones including finger bones, ankle bones and the knee cap have been shown to provide higher nuclear DNA yield rates compared to the large leg bones. Using synchrotron radiation micro-CT, researchers were able to examine segments from smaller bones to see if visible cellular spaces that house bone cells during life, called osteocyte lacunae, resulted in the greater nuclear DNA yields. The study demonstrated that microscopic traces of soft tissue between bony struts likely contributed to higher DNA yield rates from these bones. This suggests that small, easily accessible bones could provide a more efficient way of sampling hard tissues for DNA testing.



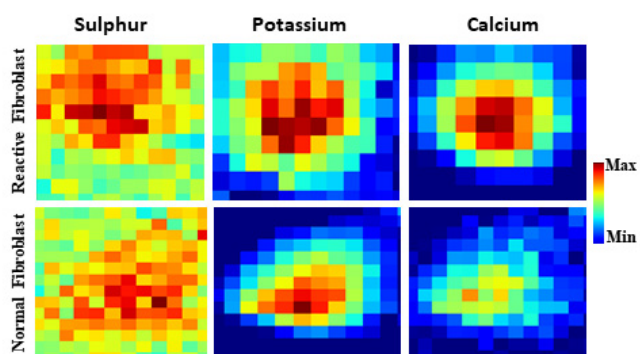
Synchrotron micro-CT cancellous bone 3D render. Soft tissue remnants (light grey) are evident between the bony struts (dark grey). Scale bar=300 μm.

Andronowski, Janna M., Amy Z. Mundorff, Isaac V. Pratt, Jon M. Davoren, and David ML Cooper. "Evaluating differential nuclear DNA yield rates and osteocyte numbers among human bone tissue types: A synchrotron radiation micro-CT approach." *Forensic Science International: Genetics* 28 (2017): 211–218.

Insights into biochemical alteration in cancer-associated fibroblasts by using novel correlative spectroscopy

Mid-IR

Understanding the biochemical changes associated with cancer growth could help improve screening and early detection techniques. Using a combination of FTIR, XAS, and XFI, researchers carried out a detailed in situ analysis of the biochemical changes in cancer-activated cells known as fibroblasts. Their work revealed both element concentrations and alterations in the chemical forms of different elements. Through IR imaging, the researchers observed for the first time that oxidative stress causes lipid degradation. This information will be used to better understand the mechanisms of cancer progression.



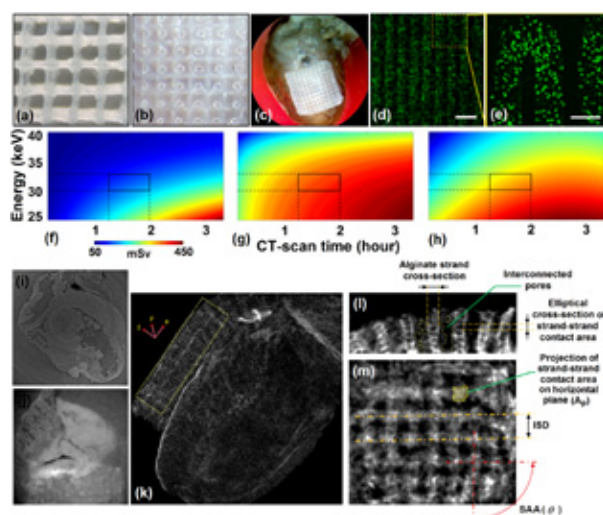
XFI elemental mapping of cancer cell lines stimulated (reactive fibroblast, upper panel) and normal fibroblast (lower panel) fibroblast. Elemental maps of S, Ca and K of a single fibroblast from both samples. Colour bar shows the concentration and localization of these elements. Each pixel is 4x4 microns in size.

Kumar, Saroj, Xia Liu, Ferenc Borondics, Qunfeng Xiao, Renfei Feng, Erik Goormaghtigh, and Fredrik Nikolajeff. "Insights into biochemical alteration in cancer-associated fibroblasts by using novel correlative spectroscopy." *ChemistryOpen* 6, no. 1 (2017): 149-157.

Potential of propagation-based synchrotron X-ray phase-contrast computed tomography for cardiac tissue engineering

BMIT

The heart cannot repair itself once it is damaged due to a heart attack, but hydrogel based bioprinted cardiac patches offer a new pathway to repairing heart tissues. Visualizing hydrogels after implantation is impossible with conventional techniques, limiting their applications so far. This work optimizes synchrotron-based phase-contrast imaging computed tomography for assessing the hydrogel patches. The technique both enhances images and minimizes the X-ray dose, without requiring the use of a contrast agent. This will make it possible to perform in vivo studies of implanted hydrogels and their microstructures, refining their use.



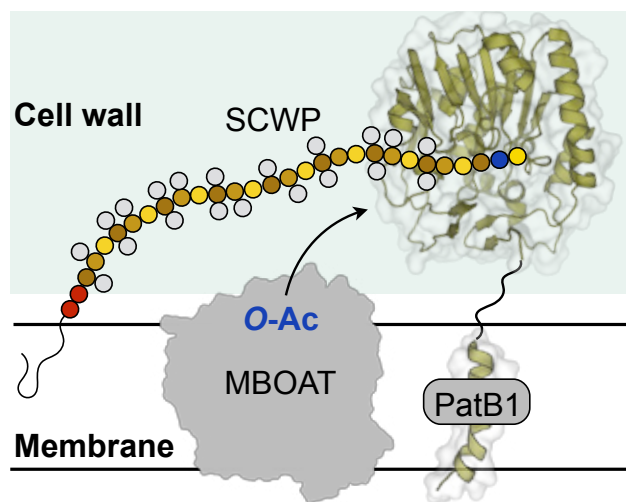
The top view of the 3D printed hydrogel implant a) in the absence of fibrin, b) with fibrin hydrogel to fill the pores and c) after implantation in-situ, where d, e) the human coronary artery endothelial cells (green dots) have been laden with the hydrogel during printing. Mapping the variation of f) dose, g) contrast to noise ratio (CNR), and h) structural similarity index (SSI) with respect to CT scan time to identify optimum ranges of X-ray energy and CT-scan time to achieve a low-dose X-ray phase contrast computed tomography (PCI-CT) for visualization of i, j) anatomical features, k) site of implantation proximal to the suture on myocardium, and l, m) quantitative assessment of microstructural features of the 3D printed cardiac implant.

Izadifar, Mohammad, Paul Babyn, Dean Chapman, Michael E. Kelly, and Xiongbiao Chen. "Potential of propagation-based synchrotron X-ray phase-contrast computed tomography for cardiac tissue engineering." *Journal of Synchrotron Radiation* 24, no. 4 (2017).

PatB1 is an O-acetyltransferase that decorates secondary cell wall polysaccharides

CMCF

Some human infections, including anthrax, are caused by certain *Bacillus* pathogens. Despite the historical significance of anthrax as a lethal human pathogen and its notoriety for being weaponized, most human *Bacillus* infections are caused by *B. cereus*. This work looks at a biosynthetic step in the assembly of *B. cereus*' cell wall to better understand the pathogen's mechanism of action and infection. It identifies the enzyme polysaccharide O-acetyltransferase (Pat) B1 as the enzyme responsible for a critical specific O-acetylation that occurs on the secondary cell polysaccharides of these pathogens; without this O-acetylation the cell wall does not form properly. Both the biochemical and structural characterization of PatB1 are presented, information that is essential if the enzyme is to be developed as a new antibacterial target. The study also provides insight into how O-acetyltransferases function to minimize, if not preclude, esterase activity.



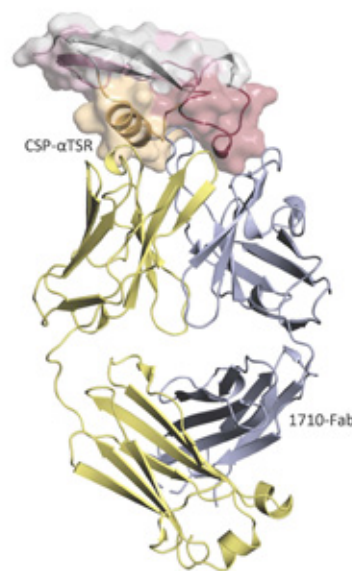
O-acetylation of secondary cell-wall polysaccharides (SCWPs). An integral membrane-bound O-acyltransferase (MBOAT), presumably PatA1, translocates an acetyl groups from a cytoplasmic source across the cytoplasmic membrane for their transfer to SCWPs by PatB1.

Sychantha, David, Dustin J. Little, Robert N. Chapman, Geert-Jan Boons, Howard Robinson, P. Lynne Howell, and Anthony J. Clarke. "PatB1 is an O-acetyltransferase that decorates secondary cell wall polysaccharides." *Nature chemical biology* 14, no. 1 (2018): 79-85.

Rare PfCSP C-terminal antibodies induced by live sporozoite vaccination are ineffective against malaria infection

CMCF

Nearly half of the world's population is at risk of malaria, a potentially lethal disease that is transmitted to people by the bites of infected mosquitos. Researchers are working to develop a malaria vaccine, many focusing on the infectious stage of *Plasmodium falciparum*, the deadliest of the species that cause malaria. In this project, researchers examined antibodies produced by volunteers who received a candidate malaria vaccine and were then exposed to the parasite to evaluate protection in a clinical trial. Researchers will be able to refine the vaccine to improve immunity to malaria with information garnered from the protein structure of these antibodies.



The crystal structure of the human non-neutralizing 1710 antibody (Fab fragment) in complex with the *Plasmodium falciparum* circumsporozoite protein α -thrombospondin type I-repeat domain (CSP- α TSR).

Scally, Stephen W., Rajagopal Murugan, Alexandre Bosch, Gianna Triller, Giulia Costa, Benjamin Mordmüller, Peter G. Kremsner, B. Kim Lee Sim, Stephen L. Hoffman, Elena A. Levashina, Hedda Wardemann, and Jean-Philippe Julien. "Rare PfCSP C-terminal Antibodies Induced by Live Sporozoite Vaccination Are Ineffective against Malaria Infection." *The Journal of Experimental Medicine* 215, no. 1 (2017): 63-75.

Structure and functional dynamics of the mitochondrial Fe/S cluster synthesis complex

CMCF

Iron-sulfur clusters are key components of many proteins critical to life, and defects in these clusters cause severe, and potentially fatal, human diseases. This study builds our understanding of how iron-sulfur clusters are created in the mitochondria, one of the primary synthesis sites. Biochemical investigation, and crystal and solution structures provide insight into both the structure and function of the protein complex responsible for creating these clusters. The results indicate that the cluster synthesis is linked with mitochondrial lipid synthesis and cellular energy.

Boniecki, Michal T., Sven A. Freibert, Ulrich Mühlenhoff, Roland Lill, and Mirosław Cygler. "Structure and functional dynamics of the mitochondrial Fe/S cluster synthesis complex." *Nature Communications* 8, no. 1 (2017): 1287.

Cystic fibrosis swine fail to secrete airway surface liquid in response to inhalation of pathogens

BMIT

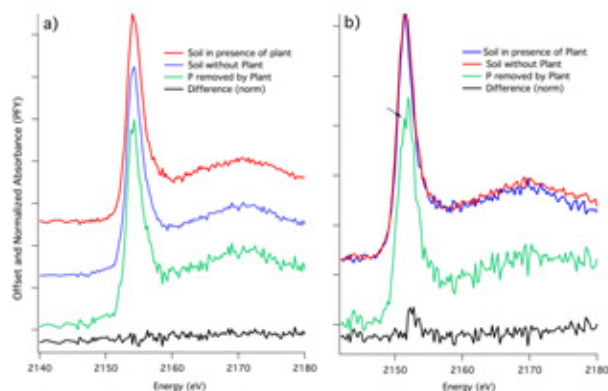
Cystic fibrosis is the most common fatal genetic disease among Canadian children and young adults. The results in this paper present clear evidence that the genetic mutation that causes cystic fibrosis prevents normal secretion of airway surface liquid, including mucus, which might lead to a cascade of infection and inflammation in lungs as the incurable disease progresses. A lack of healthy mucus makes those with the disease unable to clear bacteria from their lungs. This new insight into the disease was achieved using an in vivo PCI technique the team developed at the CLS.

Luan, Xiaojie, George Belev, Julian S. Tam, Santosh Jagadeeshan, Noman Hassan, Paula Gioino, Nikolay Grishchenko, Yanyun Huang, James L. Carmalt, Tanya Duke, Teela Jones, Bev Monson, Monique Burmester, Tomer Simovich, Orhan Yilmaz, Veronica A. Campanucci, Terry E. Machen, L. Dean Chapman, and Juan P. Iwanowski. "Cystic Fibrosis Swine Fail to Secrete Airway Surface Liquid in Response to Inhalation of Pathogens." *Nature Communications* 8, no. 1 (2017).

Effects of plant growth and time on phosphorus speciation in a manure-amended Prairie soil under controlled conditions

SXRMB

Applying livestock manure to agricultural soils is a cost-effective, nutrient-rich fertilizer. However, meeting crop nitrogen requirements with manure often leads to an overabundance of phosphorus, which can then enter water systems and stimulate undesirable algal blooms in water systems. The speciation of phosphorus in agricultural soils is affected by the presence of plants and time. Researchers used a combination of techniques including XANES to study the forms and distribution of phosphorus in a typical cultivated prairie at 1, 3, and 5 weeks after the application of cattle and hog manure. This is among the first studies that examined phosphorus forms in typical North American prairies during crop growth.



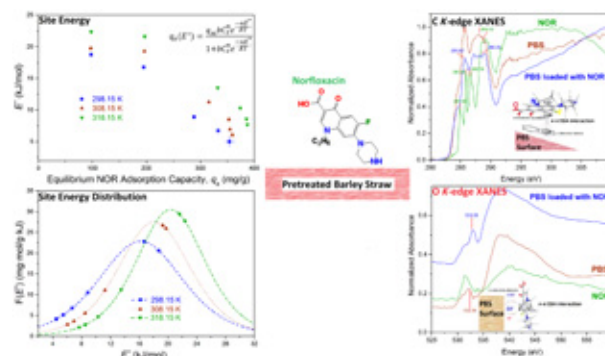
Comparison of the effect of time in a) solid cattle and b) liquid hog manure amended soil after 5 weeks of addition in the presence or absence of plant growth. The application of both manure resulted in no large changes in the bulk speciation or P crystallinity in the manured soil over the five-week period.

Kar, Gourango, David Hilger, Jeff J. Schoenau, and Derek Peak. "Effects of plant growth and time on phosphorus speciation in a manure-amended Prairie soil under controlled conditions." *Rhizosphere* 4 (2017): 1-8.

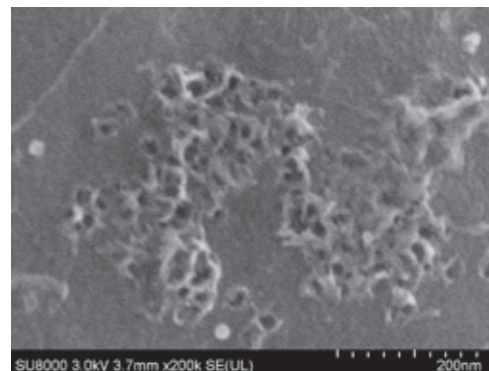
Kinetics, electron-donor-acceptor interactions, and site energy distribution analyses of norfloxacin adsorption on pretreated barley straw

SM

The presence of pharmaceuticals, and in particular antibiotics, in water systems has raised concern about risks to human health and ecosystems. Norfloxacin is a common antibiotic that has been detected in a variety of aquatic systems, and it can accumulate to high levels in soils. Raw barley straw treated with H_3PO_4 and microwave heating can be used remove norfloxacin from wastewater, preventing it from ever entering natural water systems. Pretreated barley straw works on norfloxacin via adsorption, considered one of the most effective methods to remove contaminants from aqueous systems. The results in this paper indicate that electron donor acceptor interaction was one of the dominant mechanisms for adsorption in this case.



Site energy distribution and the C and O K-edge XANES spectra



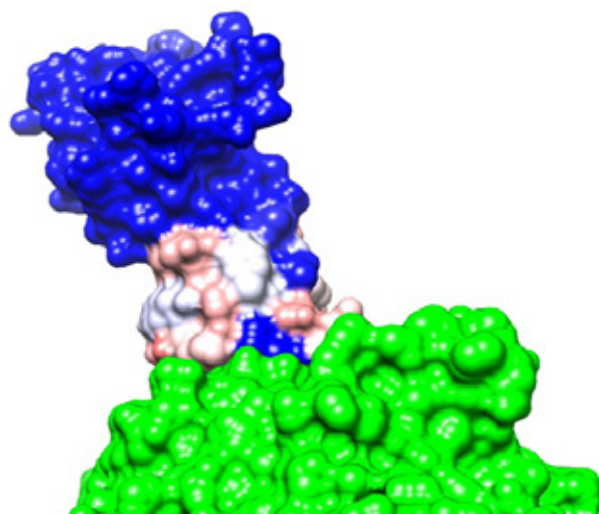
Scanning Electron Microscopy

Yan, Bei, Catherine Hui Niu, and Jian Wang. "Kinetics, electron-donor-acceptor interactions, and site energy distribution analyses of norfloxacin adsorption on pretreated barley straw." *Chemical Engineering Journal* 330 (2017): 1211-1221.

Receptor-binding loops in alphacoronavirus adaptation and evolution

CMCF

Coronaviruses cause a number of respiratory, gastrointestinal and neurological diseases in birds and mammals, including the common cold and Middle East Respiratory Syndrome (MERS). In a process known as viral adaptation, these viruses can undergo changes which allow them to infect an individual more than once. Viral adaptation is also required for the transmission of viruses, such as the coronaviruses Severe Acute Respiratory Syndrome (SARS) and MERS, from animals to humans. This study reports the X-ray crystal structure of the receptor-binding domain of one of the cold-causing coronaviruses (229E) in complex with its receptor, human aminopeptidase N. The study shows that changes in the viral receptor binding loops mediate viral adaptation, a finding relevant to understanding both immune evasion and cross-species transmission.



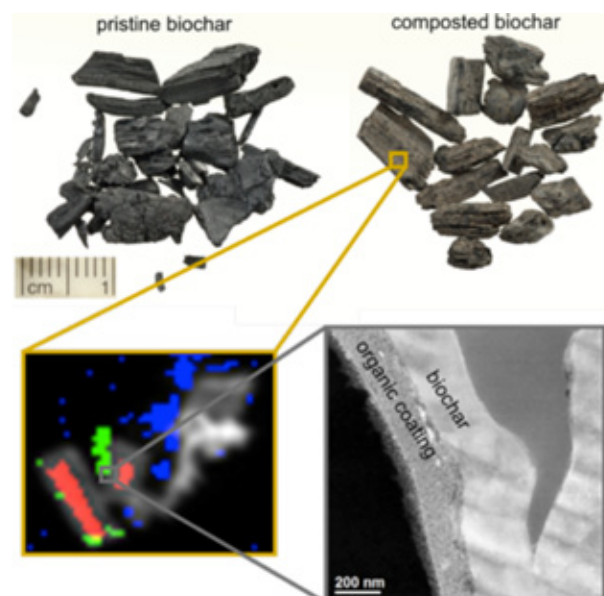
Surface representation of the human coronavirus, 229E, receptor-binding domain in complex with human aminopeptidase N. Human aminopeptidase N, coloured green; 229E receptor binding domain, red-blue colour coded to represent the natural viral sequence variation observed over the past 50 years (blue, least variation; red, greatest variation). The receptor binding loops mediate the interaction with aminopeptidase N and are the most variant.

Wong, Alan H.M., Aidan C.A. Tomlinson, Dongxia Zhou, Malathy Satkunarajah, Kevin Chen, Chetna Sharon, Marc Desforges, Pierre J. Talbot, and James M. Rini. "Receptor-binding loops in alphacoronavirus adaptation and evolution." *Nature Communications* 8, no. 1 (2017): 1735.

Organic coating on biochar explains its nutrient retention and stimulation of soil fertility

SM

Biochar, charcoal which is used as a soil amendment, both helps address climate change and soil degradation by sequestering carbon and promoting plant growth as a nutrient carrier. At CLS, researchers investigated the mechanism for the nutrient capture and slow release and identified a complex, nutrient-rich organic coating on biochar after co-composting with manure. The research, supported by nuclear magnetic resonance, XPS and scanning transmission electron microscopy analysis, suggests that the function of biochar in soil is determined by the formation of the organic coating, which enhances nutrient retention. The findings could lead to the creation of an organic slow release fertilizer with significantly better performance than current products.



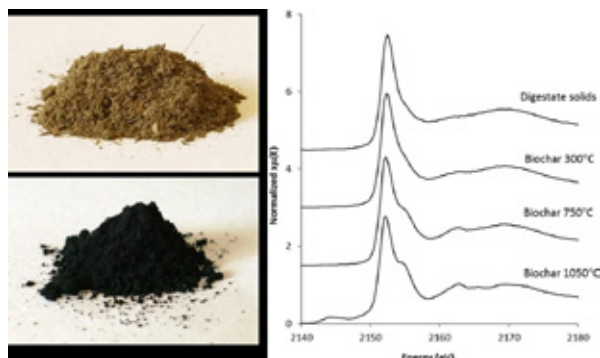
Pristine biochar as obtained from the producer and biochar after co-composting with manure. The gold inset shows data obtained by scanning transmission X-ray microscopy at CLS to identify regions rich in nutrient (blue and green). Scanning transmission electron microscopy (grey inset) shows the organic coating.

Hagemann, Nikolas, Stephen Joseph, Hans-Peter Schmidt, Claudia I. Kammann, Johannes Harter, Thomas Borch, Robert B. Young et al. "Organic coating on biochar explains its nutrient retention and stimulation of soil fertility." *Nature Communications* 8, no. 1 (2017): 1089.

The effect of different pyrolysis temperatures on the speciation and availability in soil of P in biochar produced from the solid fraction of manure

SXRMB and VLS-PGM

Charcoal, or biochar, has long been used as a fertilizer, providing a long-acting, stable, source of carbon for the soil. It is produced by pyrolysis, a heat-based decomposition in the absence of oxygen. In this paper, researchers combine XPS, scanning electron microscope and XANES spectroscopy to understand how pyrolysis temperature affects phosphorus speciation in biochar produced from solids separated from residues of anaerobic digestion. Pyrolysis had little effect on phosphorus speciation at low temperature where the phosphorus predominantly occurred as simple calcium phosphates. As the temperature increased above 600°C, the phosphorus gradually became more thermodynamically stable in species such as apatite. This change in speciation coincided with a drop in phosphorous bioavailability.



Solids of residue from anaerobic digestion to produce biogas and biochar produced from the residue. P K-edge spectra of the residue and biochar shows that calcium phosphates become increasingly condensed into apatite-like structures.

Bruun, Sander, Sarah L. Harmer, Georgios Bekiaris, Wibke Christel, Lucia Zuin, Yongfeng Hu, Lars Stoumann Jensen, and Enzo Lombi. "The effect of different pyrolysis temperatures on the speciation and availability in soil of P in biochar produced from the solid fraction of manure." *Chemosphere* 169 (2017): 377-386.

Aluminum complexation with malate within the root apoplast differs between aluminum resistant and sensitive wheat lines

SGM

Globally, it is estimated that acid soils result in more than \$161 billion in lost production annually. In acid soil conditions, roots uptake aluminum, which destroys the root system, killing the plant. Even traces of aluminum are toxic in highly acidic environments. Plants that are able to tolerate high aluminum concentrations within their tissues produce organic acids. To better understand the underlying mechanism for this resistance, researchers used XANES to conduct the first study of aluminum speciation within plant tissue.



Impact of increasing Al concentrations (right to left) on roots of wheat. Image from Steve Carr.

Kopittke, Peter M., Brigid A. McKenna, Chithra Karunakaran, James J. Dynes, Zachary Arthur, Alessandra Gianoncelli, George Kourousias et al. "Aluminum complexation with malate within the root apoplast differs between aluminum resistant and sensitive wheat lines." *Frontiers in Plant Science* 8 (2017): 1377.

Anaerobic microsites have an unaccounted role in soil carbon stabilization

SGM

If soil systems, which are among the earth's most important carbon reservoirs, release more CO₂ as temperatures change, it could lead to a positive feedback loop accelerating the effects of climate change. In order to predict whether such a feedback loop would occur, researchers need a stronger understanding of the mechanisms of carbon release from soil. This project addresses those mechanisms in anaerobic microsites, and shows that they are important regulators of soil carbon stability. This work makes it clear that anaerobic carbon protections should play an important role in climate models, though they had not previously been examined.

Keiluweit, Marco, Tom Wanzek, Markus Kleber, Peter Nico, and Scott Fendorf. "Anaerobic microsites have an unaccounted role in soil carbon stabilization." *Nature communications* 8, no. 1 (2017): 1771.

Wheat flag leaf epicuticular wax morphology and composition in response to moderate drought stress are revealed by SEM, FTIR-ATR and synchrotron X-ray spectroscopy

Mid-IR and SM

Wheat accounts for more than 20% of the world's food sources. Late-season drought conditions pose a considerable challenge for producers, a problem that may be exacerbated as global temperatures are expected to increase. This work describes a new, simple non-destructive method to screen hundreds of wheat leaf samples in a day, reducing the time and cost associated with traditional breeding programs to select varieties for drought tolerance. The team were the first to link micro and macronutrients in the leaves in relation to their ability to tolerate drought, finding higher levels of zinc in the drought-resistant wheat variety they studied.

Willick, Ian R., Rachid Lahlali, Perumal Vijayan, David Muir, Chithra Karunakaran, and Karen K. Tanino. "Wheat flag leaf epicuticular wax morphology and composition in response to moderate drought stress are revealed by SEM, FTIR-ATR and synchrotron X-ray spectroscopy." *Physiologia plantarum* (2017).

Photoperiodic regulation of growth-dormancy cycling through induction of multiple bud-shoot barriers preventing water transport into the winter buds of Norway spruce

Mid-IR

In order to survive long winters, trees in temperate and boreal zones stop growing and enter a dormant state before cold hits. This work focuses on the crown region at the base of winter buds in certain species of conifers, a plate of thick-walled cells thought to prevent ice formation in the bud. The team used mid-IR spectromicroscopy to analyze the presence and distribution of crown cell wall components in situ, providing insight into the regulatory mechanisms for growth and dormancy in conifers. This insight is important to predicting how trees may respond to climate change, which could change the timing of cues for trees to enter winter dormancy.



From the left: Shoot tip of a growing plant under long days; plant with terminal winter bud after short-day exposure for three weeks; plant with brown bud scales after short day exposure for eight weeks; plant showing bud break and new growth three weeks after re-transfer to long days following eight weeks under short days.

Lee, YeonKyeong, Chithra Karunakaran, Rachid Lahlali, Xia Liu, Karen Tanino, and Jorunn Elisabeth Olsen. "Photoperiodic regulation of growth-dormancy cycling through induction of multiple bud-shoot barriers preventing water transport into the winter buds of Norway spruce." *Frontiers in Plant Science* 8 (2017): 2109.

Evaluating changes in cell-wall components associated with clubroot resistance using Fourier Transform Infrared Spectroscopy and RT-PCR

Mid-IR

Clubroot disease is a serious threat to canola production in western Canada and many parts of the world. With a value of \$27 billion annually, canola is Canada's largest cash crop. Of the varieties of canola available to farmers, only about eight are resistant to clubroot, and these are showing signs of losing resistance to the disease. In order to develop better, multi-gene resistance in the plants, researchers used FTIR to understand changes in the composition of the root cell walls and to identify the mechanisms for clubroot resistance. Their results indicate that several cell-wall components, including lignin and pectin, may play a role in clubroot defense responses.

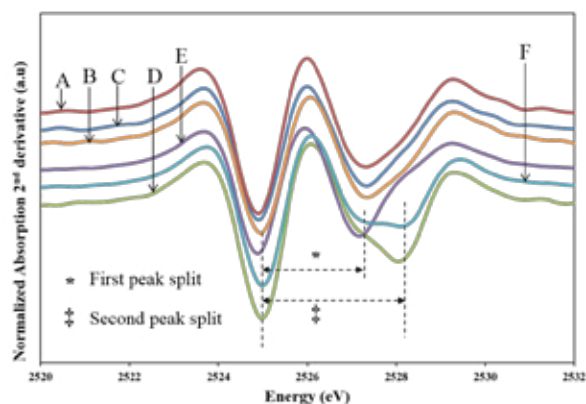
Lahlali, Rachid, Tao Song, Mingguang Chu, Fengqun Yu, Saroj Kumar, Chithra Karunakaran, and Gary Peng. "Evaluating Changes in Cell-Wall Components Associated with Clubroot Resistance Using Fourier Transform Infrared Spectroscopy and RT-PCR." *International journal of molecular sciences* 18, no. 10 (2017): 2058.

ENVIRONMENT

Insights into individual and combined effects of phosphorus and EDTA on performance of NiMo/MesoAl₂O₃ catalyst for hydrotreating of heavy gas oil

SXRMB

Increasing energy needs have led to a demand for oil from unconventional sources, such as oil sands and shale. The oil sands bitumen derived heavy gas oil can contain as much as 40,000 parts per million sulphur and 4,000 ppm nitrogen, which must be removed via hydrotreating before the heavy oil can be refined. In this work, researchers developed a catalyst with improved capacity to remove sulphur and nitrogen during the hydrotreating process, at 230% and 30% improvement over industry standards, respectively. The researchers used XANES to evaluate the catalyst's performance and function.



Catalyst understanding at molecular level using second derivative Mo L_{III}-edge XANES analysis:

- a) NiMoP/MesoAl₂O₃(MCI),
- b) MoP/MesoAl₂O₃(SI),
- c) MoP/MesoAl₂O₃(MCI),
- d) 1ENiMoP/MesoAl₂O₃(MCI),
- e) NiMoP/MesoAl₂O₃(SI) and
- f) 0.5ENiMoP/MesoAl₂O₃(MCI)

Badoga, Sandeep, Ajay K. Dalai, John Adjaye, and Yongfeng Hu. "Insights into individual and combined effects of phosphorus and EDTA on performance of NiMo/MesoAl₂O₃ catalyst for hydrotreating of heavy gas oil." *Fuel Processing Technology* 159 (2017): 232-246.

Development of shaped NiCoMg/γ-Al₂O₃ catalyst with commercial support for CO₂ reforming of CH₄

SXRMB

Methane and carbon dioxide can be converted into syngas, which can then be used to produce hydrocarbon fuels and other valuable chemicals. In order to make the conversion reaction economically viable, suitable catalysts must be identified. This project is part of an effort to develop a shaped bulk catalyst that works as efficiently as loose powders, which would be more appropriate for industrial use. Researchers in this project used XANES in conjunction with a variety of other techniques to characterize the physical and chemical properties of a new shaped catalyst towards this end.



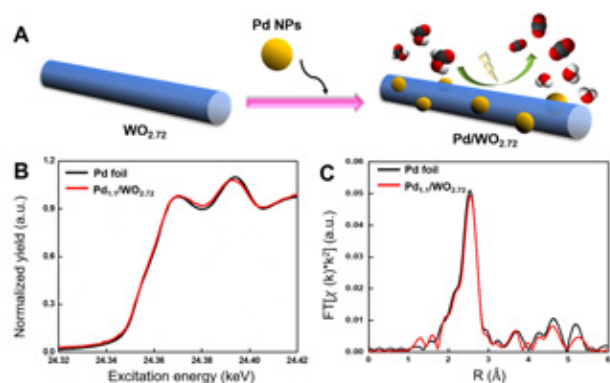
The shaped NiCoMg/γ-Al₂O₃ catalyst.

Liang, Meisheng, Lu Tian, Mohsen Shakouri, Yongfeng Hu, and Hui Wang. "Development of shaped NiCoMg/γ-Al₂O₃ catalyst with commercial support for CO₂ reforming of CH₄." *Catalysis Today* 291 (2017): 76-85.

Pd nanoparticles coupled to WO_{2.72} nanorods for enhanced electrochemical oxidation of formic acid

CLS@APS

Formic acid is a simple acid that is both abundant in nature and easily synthesized by reducing atmospheric CO₂ or from decomposing of plant cellulose. It can be used as a renewable fuel source for Direct Formic Acid Fuel Cells (DFAFCs), converting energy it stores to electric energy via an oxidation (electron-releasing) process. The key to producing commercially viable DFAFCs is to develop a robust catalyst for reactions at the cathode and anode. Using a combination of techniques, including XAS, researchers were able to develop a more efficient palladium-based anode catalyst and demonstrate an important strategy to enhance catalyst efficiency for the formic acid oxidation reaction.



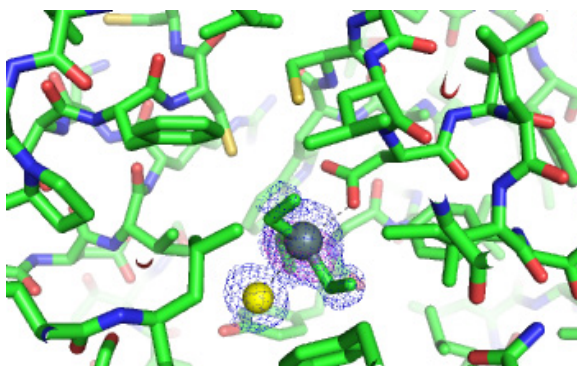
a) Schematic illustration of the strongly coupled Pd nanoparticles with WO_{2.72} nanorods for enhanced electrochemically catalytic formic acid oxidation. b) Pd K-edge XANES spectra and c) Pd K-edge extended EXAFS spectra of the coupled Pd/WO_{2.72} and the reference Pd foil, showing the special WO_{2.72} effect on Pd nanoparticles.

Xi, Zheng, Daniel P. Erdosy, Adriana Mendoza-Garcia, Paul N. Duchesne, Junrui Li, Michelle Muzzio, Qing Li, Peng Zhang, and Shouheng Sun. "Pd nanoparticles coupled to WO_{2.72} nanorods for enhanced electrochemical oxidation of formic acid." *Nano Letters* 17, no. 4 (2017): 2727-2731.

Structural and biochemical characterization of organotin and organolead compounds binding to the organomercurial lyase MerB provide new insights into its mechanism of carbon metal bond cleavage

CMCF

Many bacteria show resistance to toxic concentrations of mercury compounds including methylmercury. This resistance comes from the fact that they produce two enzymes, MerA and MerB, that actually detoxify the mercury compounds, and these enzymes are of interest as tools for the bioremediation of methylmercury contamination. Using a complement of techniques, including X-ray crystallography, the authors investigated the catalytic mechanism of MerB. By using organotin and organolead inhibitors of MerB, they were able to systematically determine the steps by which MerB is able to cleave carbon-mercury bonds. This knowledge is valuable for improving the future applications of MerB in bioremediation of mercury-contaminated sites.



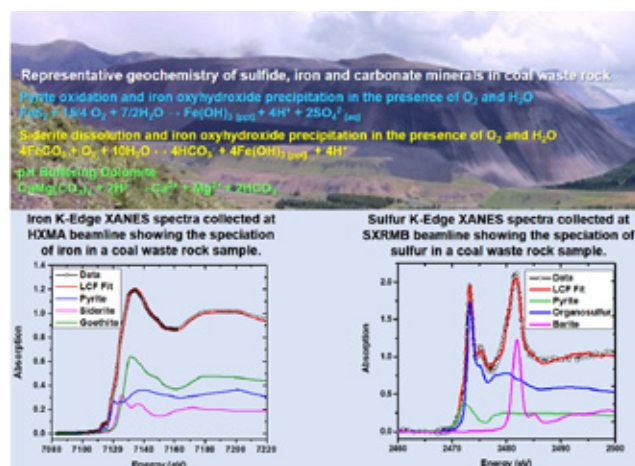
The inhibitor triethyltin bound to Asp-99 in the active site of the organomercurial lyase MerB.

Wahba, Haytham M., Michael J. Stevenson, Ahmed Mansour, Jurgen Sygusch, Dean E. Wilcox, and James G. Omichinski. "Structural and biochemical characterization of organotin and organolead compounds binding to the organomercurial lyase MerB provide new insights into its mechanism of carbon metal bond cleavage." *Journal of the American Chemical Society* 139, no. 2 (2017): 910-921.

Geochemical and mineralogical characterization of sulfur and iron in coal waste rock, Elk Valley, British Columbia, Canada

HXMA and SXRMB

The Elk River flows through a major Canadian steelmaking coal mining region, the Elk Valley. Understanding the present-day and future impacts of mining on this receiving water requires an understanding of the reactive minerals in the coal waste rock dumps, their oxidation products, as well as their oxidation and leaching rates. Potential contaminants including trace elements and sulfate released by the oxidation of sulfide minerals in coal waste rock can be transported in ground and surface waters. Researchers used a combination of techniques, including XANES, to improve our understanding of their origin, fate, and transport. Their research presents a detailed study of the evolution of iron and sulfur in coal waste rock from days old to decades, valuable information for long-term environmental health.



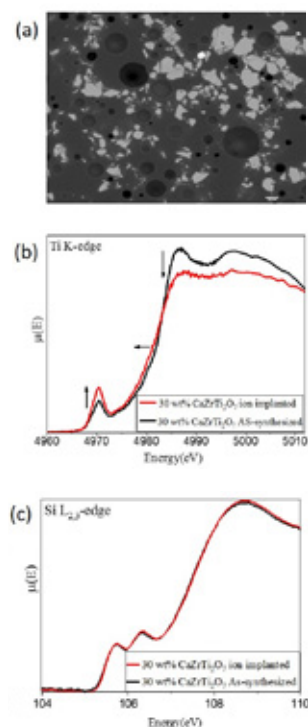
Linear combination fits of Fe and S K-edge XANES spectra for coal waste rock samples with spectra denoting the fractional contributions of respective reference compounds used to generate the fitted spectra.

Essilfie-Dughan, Joseph, M. Jim Hendry, James J. Dynes, Yongfeng Hu, Ashis Biswas, S. Lee Barbour, and S. Day. "Geochemical and mineralogical characterization of sulfur and iron in coal waste rock, Elk Valley, British Columbia, Canada." *Science of the Total Environment* 586 (2017): 753-769.

Investigation of the stability of glass-ceramic composites containing $CeTi_2O_6$ and $CaZrTi_2O_7$ after ion implantation

CLS@APS and VLS-PGM

Glass-ceramic composite materials have been investigated for nuclear waste sequestration applications due to their ability to incorporate large amounts of radioactive waste elements. How the structure of the material responds to radioactive decay is key to evaluating and developing materials for sequestration, and can be simulated by implanting high energy ions. In this work, researchers simulated radioactive decay in borosilicate glass ceramic composites and used XANES spectra to evaluate the effects on the glass matrix. They found that the glass structure of the composite materials was largely unaffected by ion implantation, but that the ceramics themselves were damaged.



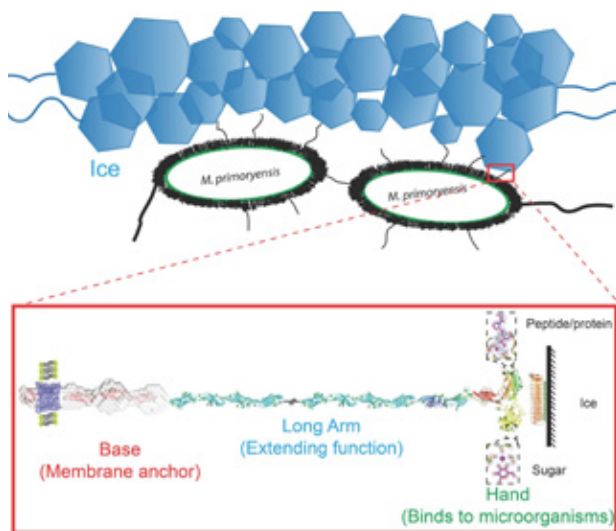
a) An electron micrograph image of a zirconolite-borosilicate glass ceramic composite (30 wt% $CaZrTi_2O_7$). b) Examination of the Ti K-edge and c) Si $L_{2,3}$ -edge XANES spectra from the materials before and after being implanted with 2 MeV Au^+ ions (dose: 5×10^{14} ions/ cm^2) are presented. The analysis of XANES spectra showed that the local environment of zirconolite was damaged as a result of ion implantation while the glass matrix remained unaffected.

Paknahad, Elham, and Andrew P. Grosvenor. "Investigation of the stability of glass-ceramic composites containing $CeTi_2O_6$ and $CaZrTi_2O_7$ after ion implantation." *Solid State Sciences* 74 (2017): 109-117.

Structure of a 1.5-MDa adhesin that binds its Antarctic bacterium to diatoms and ice

CMCF-ID

Many bacteria, including *Salmonella* and those that cause cholera, use surface protein complexes known as adhesins to bind to other surfaces and cause infections. Adhesin complexes are large and their structures repetitive, making it difficult to gather clear information about their molecular detail, leaving many fundamental questions about their function unanswered. This work was the first detailed molecular structure of a bacterial adhesin, one that binds *Marinomonas primoryensis* to ice, allowing it to better access oxygen and nutrients. This insight into adhesin action provides a vital tool for the development of inhibitors for other bacterial adhesins, potentially as treatment for chronic infections.



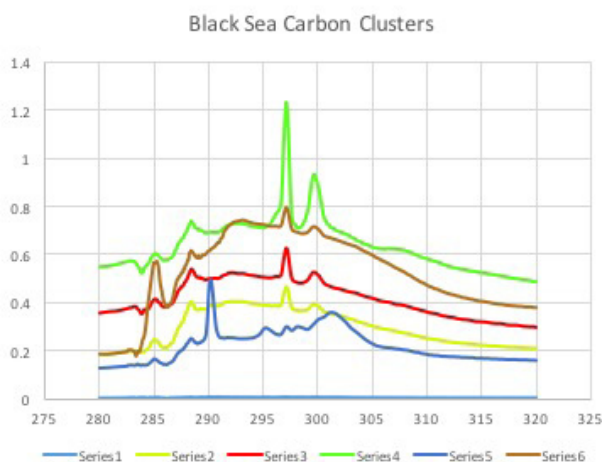
The adhesin (MplBP) is like the arm and a hand of a human being. At the base, it is attached the bacterial membrane (left), much like how an arm is attached to our body. Next it has a long arm that enables the hand on the far right to reach out and grab various things. Here, the hand of the adhesin can grip onto ice, proteins and sugars, which help the bacteria bind to ice and diatoms shown in the paper

Guo, Shuaiqi, Corey A. Stevens, Tyler DR Vance, Luuk LC Olijve, Laurie A. Graham, Robert L. Campbell, Saeed R. Yazdi et al. "Structure of a 1.5-MDa adhesin that binds its Antarctic bacterium to diatoms and ice." *Science Advances* 3, no. 8 (2017): e1701440.

Preservation of organic matter in marine sediments by inner-sphere interactions with reactive iron

SM

The world's largest carbon sinks are the oceans and the soil, with marine sediments being the largest sink for organic carbon on earth. Carbon can be bound up for thousands of years when it forms a complex with iron oxides. Given the critical role of marine sediments in the carbon cycle, iron-organic compound interactions have been extensively studied, but using model compounds. This work uses a combination of synchrotron techniques including XANES spectroscopy and STXM to provide the first examination of the actual interactions between iron and organic carbon in chemically unaltered sediments. This analysis demonstrates the importance of strong chemical bonds, called inner-sphere complexation, between iron and carbon to their long-term preservation in marine sediments.



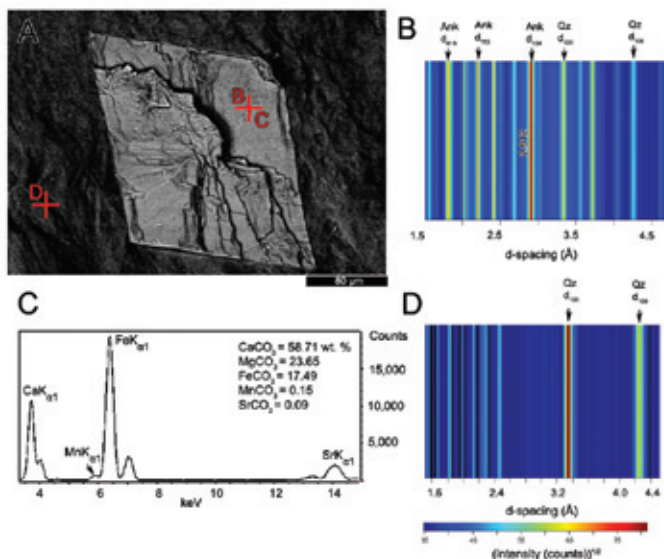
XAS spectra showing the chemical composition of different types of organic matter associated with iron in the Black Sea sediment.

Barber, Andrew, Jay Brandes, Alessandra Leri, Karine Lalonde, Kathryn Balind, Sue Wirick, Jian Wang, and Yves Gélinas. "Preservation of organic matter in marine sediments by inner-sphere interactions with reactive iron." *Scientific Reports* 7, no. 1 (2017): 366.

Uranium(IV) adsorption by natural organic matter in anoxic sediments

SM

As a fuel source uranium is an important alternative to fossil fuels, and Canada is the second largest producer and exporter of uranium in the world. In order to ensure the long term health of uranium mining sites, researchers are working to characterize the chemical form of uranium and develop models for uranium biochemistry. This work uses EXAFS, STXM, and nano-secondary ion mass spectrometry to understand uranium speciation in field-relevant conditions. The results show that uranium (IV) is adsorbed to natural organic matter in these conditions, forming a complex natural matrix.



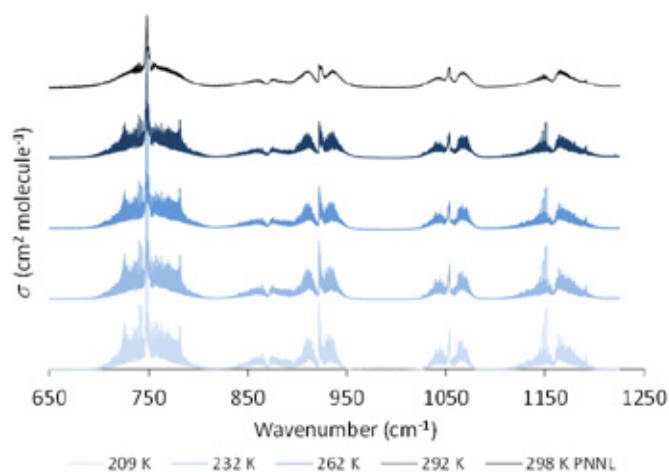
a-c) Synchrotron-based analyses shed light on the elusive paragenetic history of Fe-rich member of the dolomite series occurring within d) cherty matrices of ca. 1.88 Ga stromatolites of the Gunflint Formation (Ontario). The combination of standard spectroscopic techniques, and in situ XRF and micro XRD has demonstrated that caution must be exercised when interpreting the chemistry of carbonate phases within ancient stromatolites as paleomarine proxies. Further advances in micro-focusing technology, capable of resolving submicron-scale analytical areas, will permit future investigations of carbonate phases with origins that have previously been identified as primary to early diagenetic.

Bone, Sharon E., James J. Dynes, John Cliff, and John R. Bargar. "Uranium (IV) adsorption by natural organic matter in anoxic sediments." *Proceedings of the National Academy of Sciences* 114, no. 4 (2017): 711-716.

Infrared absorption cross sections of propane broadened by hydrogen

Far-IR

Propane is mainly produced as a by-product of natural gas processing and petroleum refining, and a small amount is created from biomass burning, oceans and volcanoes. Reliable spectra of gases like propane are valuable for atmospheric models, both on Earth and to understand the compositions of gas giant planets and exoplanets. It is difficult to attain clear spectroscopic line parameters to identify propane at cool and ambient temperatures; as an alternative, this research defines high-resolution FTIR cross-sections to be used in atmospheric observations.



A comparison of propane cross-sections broadened with 4 kPa of H₂ recorded at cold temperatures. The top trace represents the reference data taken from the Pacific Northwest National Laboratory database.

Wong, A., R. J. Hargreaves, B. Billingham, and P. F. Bernath. "Infrared absorption cross sections of propane broadened by hydrogen." *Journal of Quantitative Spectroscopy and Radiative Transfer* 198 (2017): 141-144.

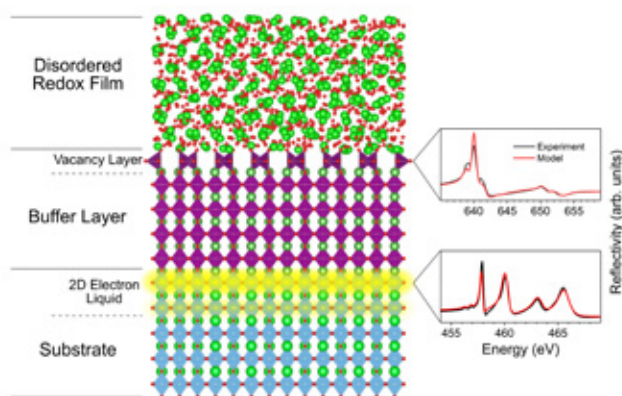


ADVANCED MATERIALS

Tuning the two-dimensional electron liquid at oxide interfaces by buffer-layer-engineered redox reactions

REIXS

Two dimensional electron liquids at oxide interfaces exhibit remarkable properties like superconductivity, magnetism, and electronic correlations. As such, these systems are highly studied and show potential for next generation electronic, magnetic and spintronic devices. Researchers have discovered a way to tune the electron liquid at oxide interfaces through a combination of ordered oxygen vacancies and polarity-induced electronic reconstruction. Resonant X-ray reflectometry experiments allowed the researchers to probe the oxygen vacancies and the electronic reconstruction at the atomic level, providing crucial insight into the mechanisms which yield ultra-high mobility 2D electron liquids.



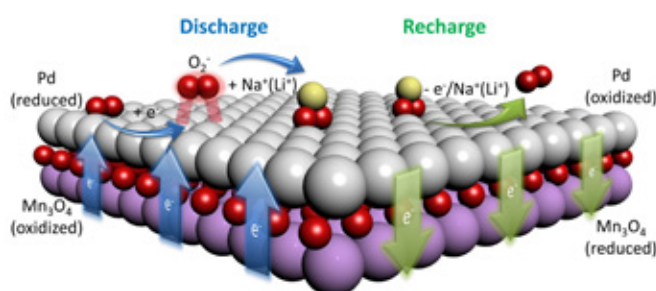
A tri-layer oxide film structure was studied with resonant reflectivity at the REIXS beamline. Researchers found that the disordered capping layer film induced ordered oxygen vacancies at its interface to a buffer layer film. These vacancies altered the polarity of the buffer layer, yielding the generation of a very high mobility 2D electron liquid at the lower interface to the substrate. The reflectivity experiments at REIXS were pivotal in disentangling these effects of multiple interfaces.

Chen, Yunzhong, Robert J. Green, Ronny Sutarto, Feizhou He, Søren Linderroth, George A. Sawatzky, and Nini Pryds. "Tuning the two-dimensional electron liquid at oxide interfaces by buffer-layer-engineered redox reactions." *Nano Letters* 17, no. 11 (2017): 7062-7066.

A bifunctional solid state catalyst with enhanced cycling stability for Na and Li-O₂ cells: revealing the role of solid state catalysts.

HXMA and SGM

Lithium- and sodium-oxygen batteries have great potential as the next generation energy storage devices, providing the highest energy densities among all the available systems. However, their applications are currently limited by several factors, including their low energy efficiency and limited lifespan. Considerable research has developed solid state catalysts that help to extend the working life of these cells, but little is known about the working mechanisms of these catalysts. This work presents detailed XANES spectroscopic analysis of the mechanism of catalytic activity in lithium and sodium cells, revealing evidence that catalysts with higher oxygen-bonding capabilities may have better catalytic ability in the cells.



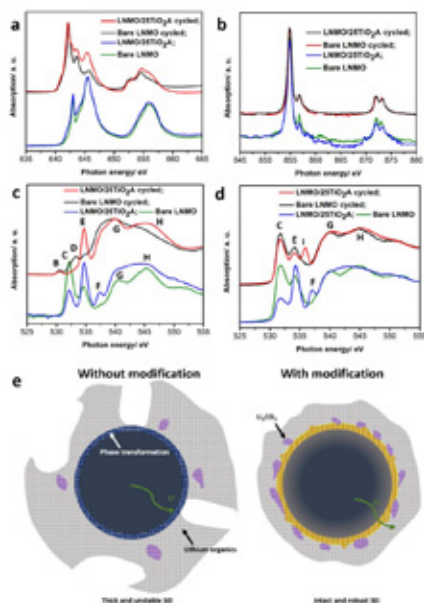
Schematic diagram of catalytic mediated discharge and charge reaction mechanisms of Li/Na-O₂ cells on the Mn₃O₄/Pd surface.

Yadegari, Hossein, Mohammad Norouzi Banis, Andrew Lushington, Qian Sun, Ruying Li, Tsun-Kong Sham, and Xueliang Sun. "A bifunctional solid state catalyst with enhanced cycling stability for Na and Li-O₂ cells: revealing the role of solid state catalysts." *Energy & Environmental Science* 10, no. 1 (2017): 286-295.

Nanoscale manipulation of spinel lithium nickel manganese oxide surface by multisite Ti occupation as high-performance cathode

SGM and SXRMB

There is a huge demand for lithium-ion batteries for electric vehicles, in large part because they are lightweight and provide high energy densities. However, in order to achieve higher mileage per charge, higher voltage and energy density cathode materials must be found. In this work, researchers successfully modified the surface structure of the high-voltage cathode material $\text{LiNi}_{0.5}\text{Mn}_{1.5}\text{O}_4$ using atomic layer deposition to boost its performance. The team used XANES spectra to characterize the samples throughout the work. These results provide new insight into the application of atomic layer deposition for better design of cathode materials.



XANES spectra of the bare LNMO, LNMO/25TiO₂A, and bare LNMO after 350 charge/discharge cycles and LNMO/25TiO₂A after 350 charge/discharge cycles in

- a) Mn $L_{2,3}$ -edges collected at TEY mode;
- b) Ni $L_{2,3}$ -edges collected at TEY mode;
- c) O K-edges collected at TEY mode;
- d) O K-edges collected at FLY mode;

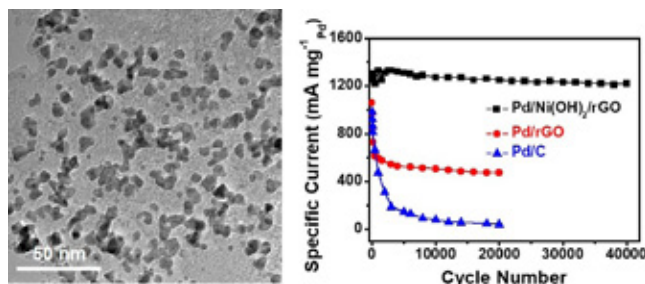
e) schematic illustration of the bare LNMO and LNMO/25TiO₂A after 350 charge/discharge cycles.

Xiao, Biwei, Hanshuo Liu, Jian Liu, Qian Sun, Biqiong Wang, Karthikeyan Kaliyappan, Yang Zhao, Mohammad Norouzi Banis, Yulong Liu, Ruying Li, Tsun-Kong Sham, Gianluigi A. Botton, Mei Cai, and Xueliang Sun. "Nanoscale Manipulation of Spinel Lithium Nickel Manganese Oxide Surface by Multisite Ti Occupation as High-Performance Cathode." *Advanced Materials* 29, no. 47 (2017): 1703764.

Promoting effect of $\text{Ni}(\text{OH})_2$ on palladium nanocrystals leads to greatly improved operation durability for electrocatalytic ethanol oxidation in alkaline solution

VESPERS

Ethanol can be produced in large quantities from renewable biomass, has a low toxicity, and burns more cleanly than petroleum, all of which makes it an attractive fuel source. Additionally, it is capable of delivering higher energy density than other alternative liquid fuels, such as formic acid and methanol. The adoption of direct ethanol fuel cells has been slowed by the lack of a viable, durable electrocatalyst for the fuel cells anode. This team developed a new strategy for the rational design of hybrid electrocatalysts for ethanol fuel cells, and produced an extremely durable hybrid catalyst.



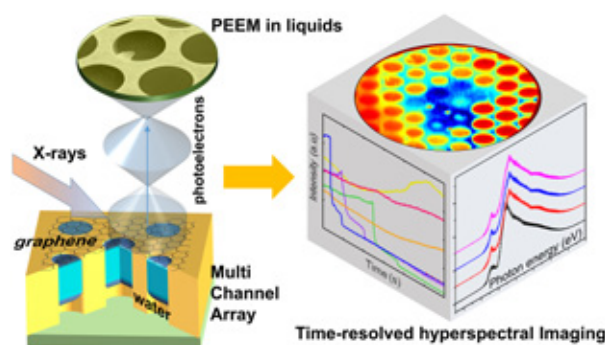
TEM image of the Pd-Ni(OH)₂-graphene hybrid electrocatalyst (left) and its cycling stability for electrocatalytic ethanol oxidation in comparison with other palladium-based electrocatalysts (right).

Huang, Wenjing, Xian-Yin Ma, Han Wang, Renfei Feng, Jigang Zhou, Paul N. Duchesne, Peng Zhang et al. "Promoting effect of $\text{Ni}(\text{OH})_2$ on palladium nanocrystals leads to greatly improved operation durability for electrocatalytic ethanol oxidation in alkaline solution." *Advanced Materials* 29, no. 37 (2017).

Enabling photoemission electron microscopy in liquids via graphene-capped microchannel arrays

SM

Solid-liquid interfaces are important in a wide range of scientific fields, including electrochemistry, geochemistry, catalysis, and biomedicine. X-ray photoemission electron microscope (PEEM) is an X-ray microscopy technique that provides detailed spatial and chemical information at a resolution of 50 nm. The technique is a powerful tool for understanding surface processes, but is traditionally limited to use under high vacuum. In this paper, researchers describe a novel liquid sample platform which employs a graphene membrane to separate the vacuum and high-pressure sample environment. This will allow researchers to use standard PEEM imaging setup to study the solid-liquid and solid-gas interfaces.



The schematics of the PEEM and graphene capped multichannel array liquid cell setups. PEEM image of the liquid interface constitutes spatial-spectro-temporal multi dimensional dataset which can be analyzed using modern data mining algorithms; (with permission from *Nano Lett.*, 2017, 17 (2), pp 1034–1041; Copyright (2017) American Chemical Society).

Guo, Hongxuan, Evgheni Strelcov, Alexander Yulaev, Jian Wang, Narayana Appathurai, Stephen Urquhart, John Vinson, Subin Sahu, Michael Zwolak, and Andrei Kolmakov. "Enabling photoemission electron microscopy in liquids via graphene-capped microchannel arrays." *Nano Letters* 17, no. 2 (2017): 1034-1041.

High-performance reduced graphene oxide-red phosphorous composites anodes for lithium batteries and soft X-ray absorption near-edge structure studies

IDEAS and VLS-PGM

Increasing green energy demands mean there is a need for better lithium ion batteries for energy storage. Red phosphorous, which is relatively cheap and abundant, and is believed to contain more energy for the same battery size, is one of the materials being explored for lithium ion battery anodes. However, phosphorous anodes currently have a poor lifetime, limiting their use. This work describes a method to create a carbon-phosphorus compound anode which delivers better storage capacity and been recharged faster. The electronic and chemical structures effect on battery performance was characterized with XANES.

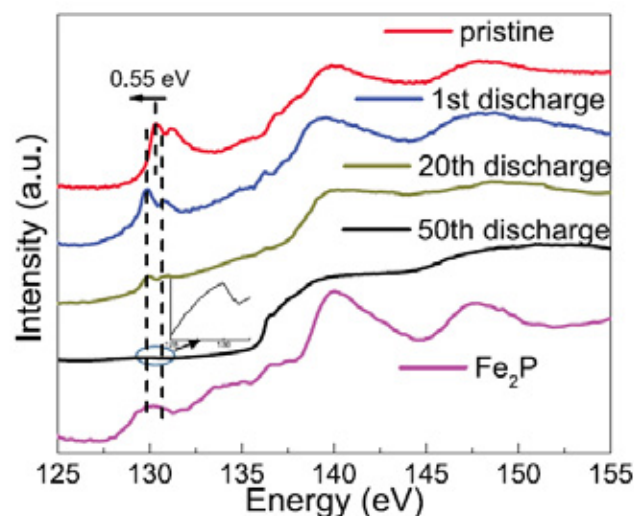


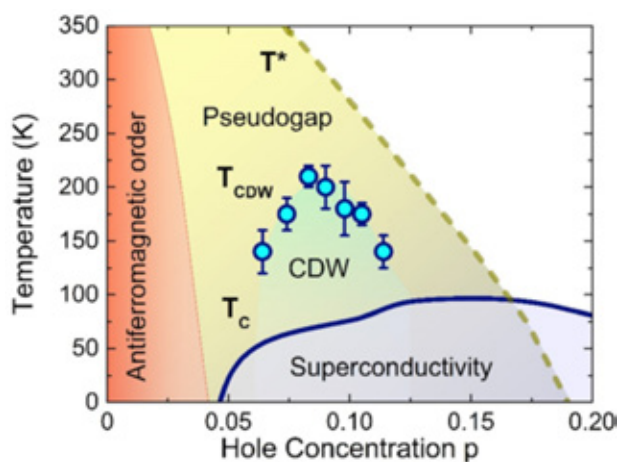
Figure 1 P $L_{2,3}$ -edge FLY XANES spectra of Fe_2P , pristine carbon-phosphorous and carbon-phosphorous electrodes discharged at different cycles. The inset indicates the trace of resonances.

Wang, Dongniu, Lucia Zuin, and David Muir. "High-performance reduced graphene oxide–red phosphorous composites anodes for lithium batteries and soft X-ray near-edge structure studies." *Canadian Journal of Chemistry* 95, no. 11 (2017): 1178-1182.

Synchrotron X-ray scattering study of charge-density-wave order in $\text{HgBa}_2\text{CuO}_{4+\delta}$

REIXS

High-temperature copper-oxide superconductors conduct electricity without energy loss at unusually high temperatures (of about 100K) and are used in a wide range of applications, including Magnetic Resonance Imaging. However, the origin of these complex materials' superconductivity is still unknown. In order to better understand the electronic properties of these quantum materials, a systematic RXS study of charge-density-wave order, which competes with the superconductivity, was performed in the model compound $\text{HgBa}_2\text{CuO}_{4+\delta}$. This work reveals that charge-density-wave order diminishes as superconductivity is optimized with increasing hole concentration, and it provides a direct link between the charge-order phenomenon and the reconstruction of the Fermi surface observed in high magnetic fields.



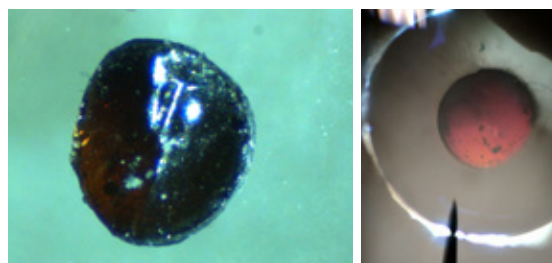
Temperature-doping phase diagram of $\text{HgBa}_2\text{CuO}_{4+\delta}$. The onset of the CDW wave order at T_{CDW} is marked by blue circles. These charge correlations are observed already above the critical temperature T_c for superconductivity, yet they only extend over a limited hole doping range.

Tabis, W., B. Yu, I. Bialo, M. Bluschke, T. Kolodziej, A. Kozłowski, E. Blackburn et al. "Synchrotron X-ray scattering study of charge-density-wave order in $\text{HgBa}_2\text{CuO}_{4+\delta}$." *Physical Review B* 96, no. 13 (2017): 134510.

X-ray induced synthesis of a novel material: Stable, doped solid CO at ambient conditions

Far-IR, HXMA, and Mid-IR

A stable solid, or polymeric, carbon monoxide could be used as a carbon dioxide storage material, thus helping to combat climate change. It could equally be used as a novel material for technological applications. Solid CO is formed under extremely high pressure; this work demonstrates a new technique for producing a stable solid CO, doped with strontium carbonate, using hard X-ray irradiation. IR spectra and EXAFS analysis helped demonstrate that the material is stable at ambient conditions, trapping CO_2 for over one year, a vast improvement over the days that pure solid CO normally survives.



Doped solid CO recovered at ambient conditions.

Pravica, Michael, Egor Evlyukhin, Petrika Cifligu, Blake Harris, Jung Jae Koh, Ning Chen, and Yonggang Wang. "X-ray induced synthesis of a novel material: Stable, doped solid CO at ambient conditions." *Chemical Physics Letters* 686 (2017): 183-188.

Novel electrospun gas diffusion layers for polymer electrolyte membrane fuel cells: Part II. In operando synchrotron imaging for microscale liquid water transport characterization

BMIT

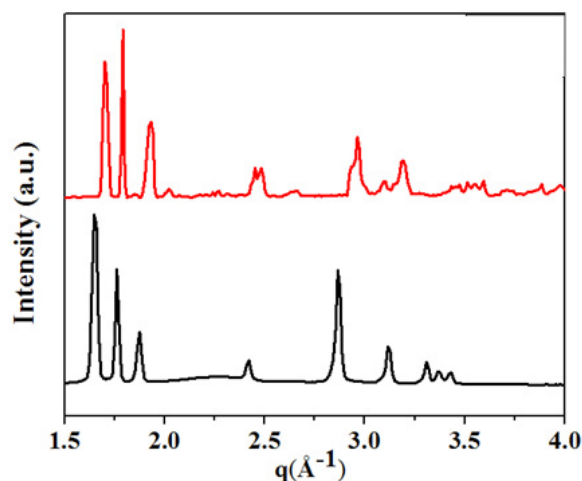
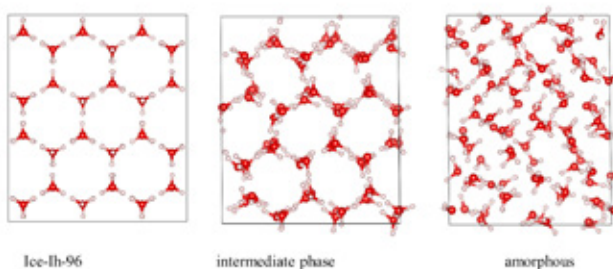
An important green technology, polymer electrolyte membrane (PEM) fuel cells use hydrogen and oxygen to produce electricity, producing only heat and water as by-products. The gas diffusion layer (GDL) provides transport pathways for reactants and products, like liquid water, which is necessary to the fuel cell's operation. However, excess water buildup in the cell can degrade its performance. Researchers used concurrent synchrotron X-ray radiography and electrochemical impedance spectroscopy in order to visualize the effect of the GDL's structure on water transport, under realistic conditions, in high spatial and time resolution. Combined with a controlled method for GDL production, this work helps optimize GDL performance for PEM fuel cells.

Chevalier, S., N. Ge, J. Lee, M. G. George, H. Liu, P. Shrestha, D. Muirhead, N. Lavielle, B. D. Hatton, and A. Bazylak. "Novel electrospun gas diffusion layers for polymer electrolyte membrane fuel cells: Part II. In operando synchrotron imaging for microscale liquid water transport characterization." *Journal of Power Sources* 352 (2017): 281-290.

Kinetically controlled two-step amorphization and amorphous-amorphous transition in ice

HXMA

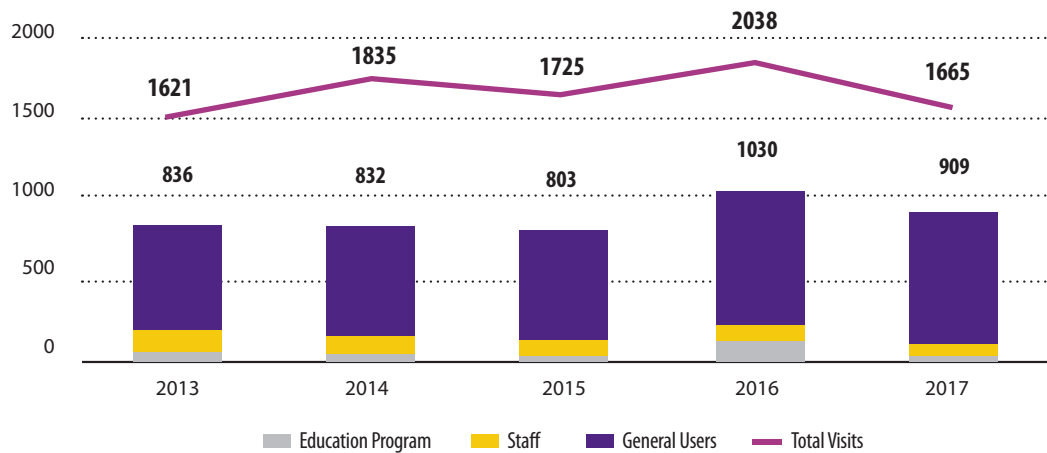
When ice is compressed at low temperatures, instead of transforming into a high-pressure crystalline form where the atoms are organized into a lattice pattern, the ice converts to an amorphous solid with disorganized atoms. Through angle dispersive XRD, this group showed that the resulting disorganized state is an intermediate crystalline phase, not a liquid. The crystalline phase is a shear-distorted form of ice, with a shifted oxygen atom. This is the first in situ structural characterization of ice under high pressure, and outlines the phase transitions of both compressed ice and decompressed amorphous ice.



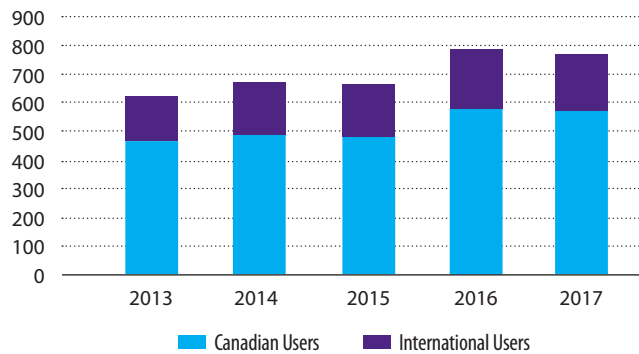
Lin, Chuanlong, Xue Yong, S. Tse John, Jesse S. Smith, Stanislav V. Sinogeikin, Curtis Kenney-Benson, and Guoyin Shen. "Kinetically controlled two-step amorphization and amorphous-amorphous transition in ice." *Physical Review Letters* 119, no. 13 (2017): 135701.

FACTS AND FIGURES

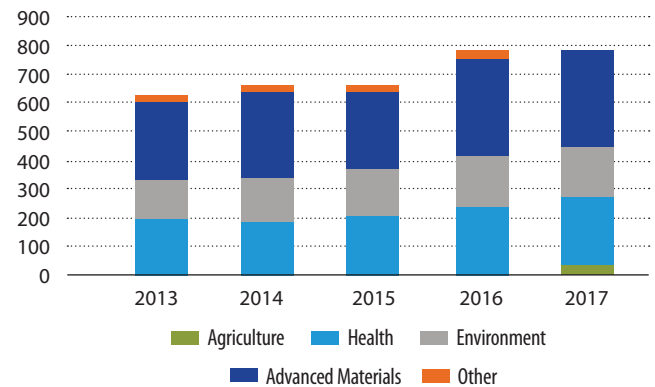
USERS AND USER VISITS



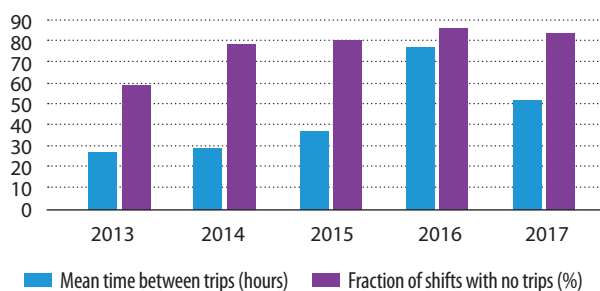
GEOGRAPHIC DISTRIBUTION OF USERS



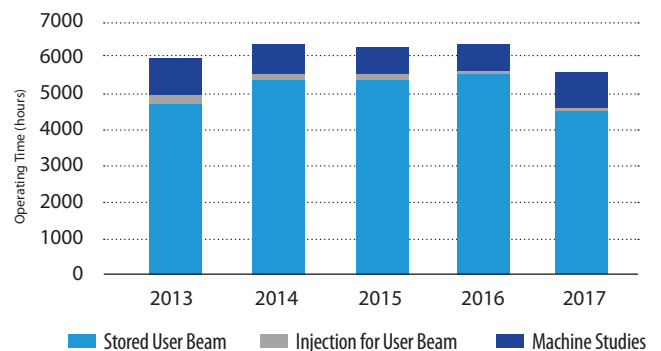
GENERAL USERS BY DISCIPLINE



STORAGE RING USER BEAM RELIABILITY



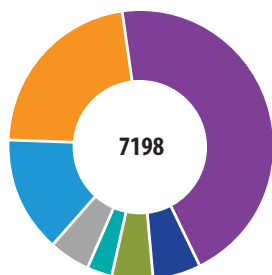
ANNUAL HOURS OF OPERATION



OVERSUBSCRIPTION

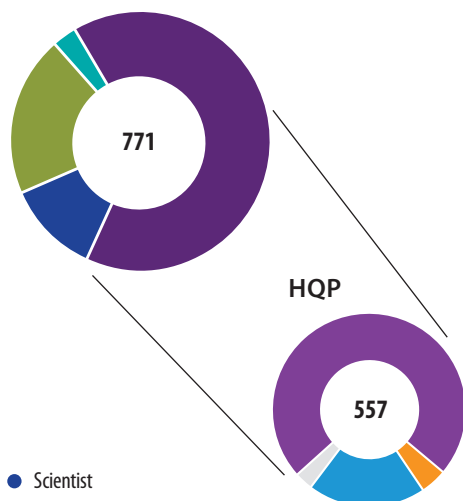
	2013	2014	2015	2016	2017
Number of Shifts Requested	4788	4921	5609	5682	5644
Shifts Allocated	3077	3082	3343	3742	2946
Oversubscription	56%	60%	68%	52%	98%
Number of Beamlines Participating	10	10	11	11	11

SHIFTS DELIVERED BY CATEGORY



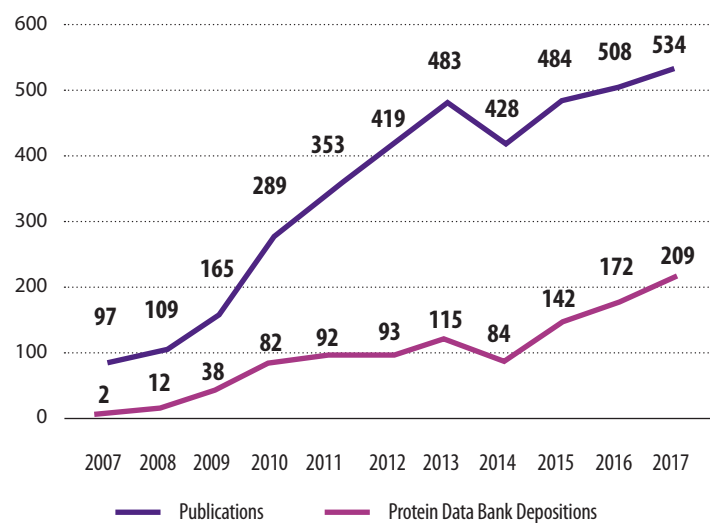
- General User - 45%
- Beamteam Member - 6%
- Purchased Access - 5%
- Special Requests - 3%
- Beamline Scientist - 5%
- Beamline Maintenance and Upgrades - 14%
- LOI/Commissioning - 22%

CLASSIFICATION OF USERS

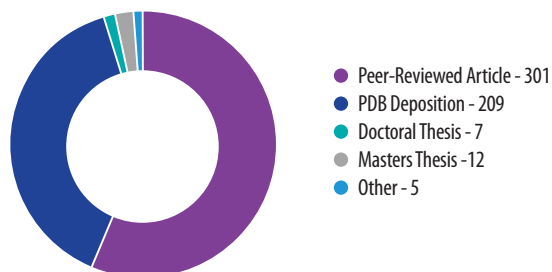


- Scientist
- Faculty
- Other Non-HQP
- Student (Undergraduate, Graduate)
- Post Doc
- Technical/Professional
- Other HQP

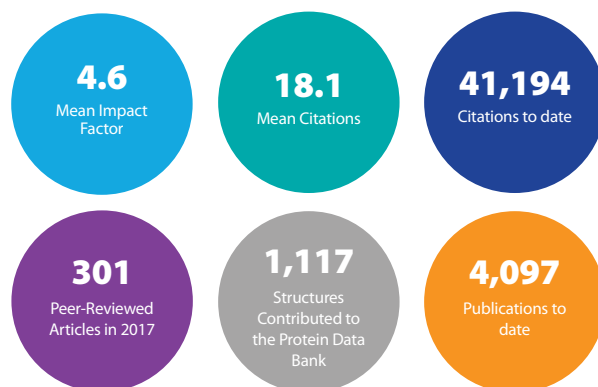
PUBLICATIONS BY YEAR



OVERALL 2017 ACTIVITY BY PUBLICATION TYPE



PUBLICATIONS



For the complete list of CLS publications, visit uso.lightsource.ca/publications



PHASE THREE **BEAMLINES**

Brockhouse X-ray Diffraction and Scattering Sector

Source	Undulator	Wiggler	
Energy Range (keV)	5-24	7-22	20-94
Wavelength (Å)	2.47-0.52	1.77-0.56	0.62-0.13
Resolution ($\Delta E/E$)	10^{-2} - 10^{-4}	3×10^{-4}	3×10^{-3}
Flux (photons/sec)	10^{14} - 10^{11}	$>10^{12}$	10^{13} - 10^{11}
Minimum Spot Size	$20 \times 170 \mu\text{m}$	$0.1 \times 0.5 \text{ mm}$	$0.25 \times 5 \text{ mm}$

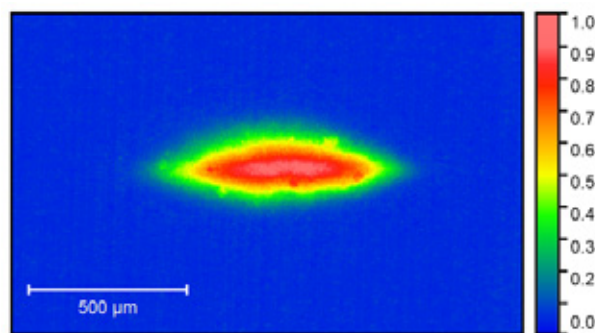
Introduction:

Brockhouse is a suite of three beamlines dedicated to using hard X-rays for diffraction and scattering techniques for material science. Two beamlines have a wiggler source and the third beamline has an undulator source. We will offer a wide range of complementary techniques for structural characterization, including high resolution powder diffraction, small molecule crystallography, total scattering to produce the pair distribution function, micro-single crystal diffraction, high pressure setups, anomalous/magnetic diffraction, low angle X-ray reflectivity, grazing incidence diffraction, and inelastic scattering. There is also a highly specialized endstation from IBM that allows diffraction experiments with temperature control up to 1100°C, ultra-high purity nitrogen or helium atmospheres, and in-situ roughness and resistance probes for the characterization of thin films.

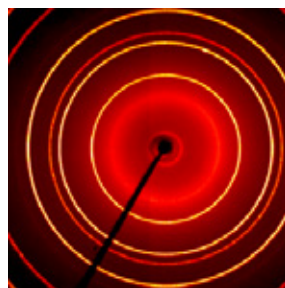


Current State:

The low energy wiggler endstations are under commissioning and will be accepting Letters of Intent proposals shortly. The high energy wiggler endstations have begun commissioning and should enter the LOI stage in a few months. Construction of the undulator beamline has begun and it should begin commissioning in a little under a year.

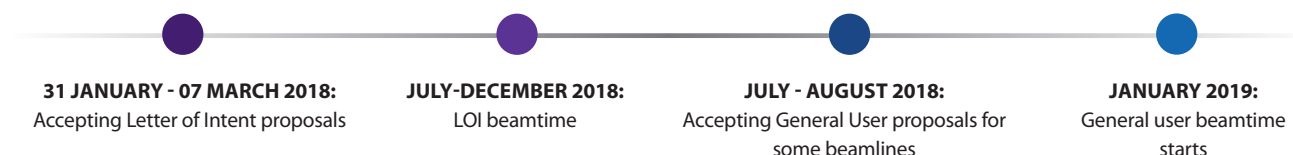


The shape of the beam spot from the <111> Si monochromator in the low energy wiggler beamline.



Diffraction pattern of Al_2O_3 on the Bruker endstation.

Estimated Timeline:



BioXAS

Bio-X-ray Absorption Spectroscopy

Introduction:

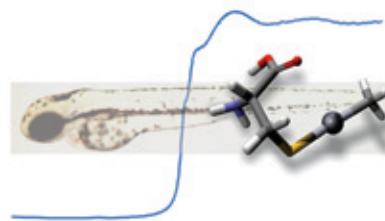
The BioXAS-Spectroscopy Centre is a suite of two beamlines specifically tailored for supporting life and environmental sciences studies using X-ray Absorption Spectroscopy. XAS is a non-destructive, bulk sensitive, element specific technique that proves to be a handy probe of the local atomic structure.

Due to the wide range of potential applications XAS beamlines are in high demand, so the recent opening of two XAS endstations at the CLS is intended to ease the access to the popular technique for the local and nationwide scientific community. The experimental procedure is simple: there is usually no need to specially prepare the surface of the sample, freeze it to low temperatures or think about crystallinity; nevertheless XAS is powerful enough to reveal the information about the chemical state of the absorbing atom, its geometry and the contents of its surroundings.

XAS works well on poorly ordered amorphous materials and due to its resonant nature the technique is sensitive to very low (down to several parts per million) concentrations of the element of interest. It helps chemists observe the evolution of catalysts in the course of reaction and modification of the lithium battery electrode during the charge/discharge cycle. Physicists use XAS to uncover the subtle changes of



lattice symmetry in complex materials invisible in regular X-ray diffraction. The technique can identify trace amounts of pollutants in water and soil and identify their origin and chemical activity. And, of course, all of the above cases find applications in the life sciences: to detect the oxidation state and preferred bonding of the metals in the proteins at low level or to see how living organisms accumulate heavy metals in their tissues and how it affects their metabolism.



XAS allows determination of the molecular form of the element of interest in intact biological tissues

Current State:

	Main	Side
Energy range (keV)	5-32	5-32
Flux (photons/s)	1012	1011
Beam spot on sample	3 x 0.5 mm	3 x 0.5 mm
Energy resolution ($\Delta E/E$)	$<10^{-4}$	$<10^{-3}$
Detectors (transmission)	20 x 170 μm	0.1 x 0.5 mm
Detectors (fluorescence)	Ion Chambers (N_2 flow, 12 cm long)	Ion Chambers (N_2 flow, 12 cm long)
Sample environment	2x Canberra HPGE 32-Channel, PIPS diode	Canberra HPGE 32-Channel, PIPS diode
Sample size	10 x 10 cm (in air), 2 x 2 cm in the cryostat	10 x 10 cm (in air), 2 x 2 cm in the cryostat

Estimated Timeline:

The beamline is in the final phase of commissioning and accepting the Letter of Intent proposals under BioXAS-Spectroscopy. The best suited endstation will be assigned upon a review.



Quantum Materials Spectroscopy Centre

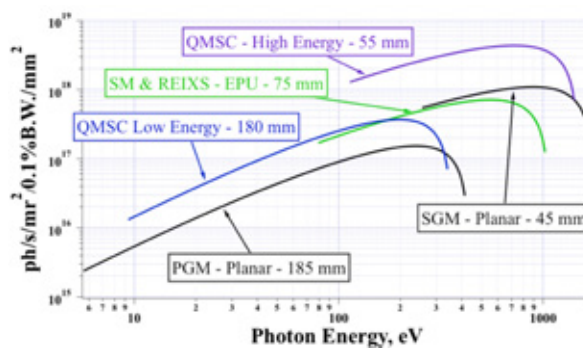
Energy range (photons/s)	15-1200 eV
Flux (photons/s)	101 -1013 (photons/s)
Beam spot on sample	20 × 100 μm
Resolving power (E/ΔE)	>104 over the full energy range
ARPES Detector	Scienta R4000
Spin + ARPES Detector	Scienta DA30
Sample environment temperature range	5-300 K

Introduction:

The Quantum Materials Spectroscopy Centre uses a unique dual-undulator as the source for investigating novel and fundamentally important materials in condensed matter physics. Both undulators are elliptically polarizing, allowing for an arbitrary orientation of light polarization. They additionally cover separate energy ranges to maximize the spectral flux over the complete range available (15-1000 eV) for the endstations. The two beamline endstations are designed for both angle-resolved photoemission (ARPES) and spin-resolved photoemission (SARPES) experiments. Additional deposition chambers will be available to create samples in-situ for analysis. These experimental setups will allow for probing the low-energy electronic state of materials. With this detailed information it becomes possible to examine many of the interesting questions generated by the correlated motion of electrons in materials.



QMSC Dual-EPU installed in the storage ring



Brilliance curves for QMSC

Current State:

There are four milestones to reach before general user experiments will be available. These commissioning milestones are a fully working dual-elliptical polarizing undulator, completed beamline and optics, and two fully operating endstations (ARPES and SARPES). Installation of the dual-EPU in the storage ring occurred in the spring of 2017. Further work is ongoing to reach complete polarization control for all of the required beamline energies. This work will progress in stages with completion scheduled for spring 2019. The beamline is currently fully assembled with a working monochromator. Only minor alignment tweaks are still needed to optimize flux to both endstations. The ARPES endstation is installed and ready for cryostat testing. The SARPES endstation is designed and currently being built. Once these milestones have been achieved the beamline will provide a uniquely capable research center for both fundamental and applied quantum materials research.

Estimated Timeline:



INNOVATIONS

The CLS offers high resolution, quality data and personalized service with a range of options from data collection to complete analysis and reporting to meet your needs.

The CLS Industrial Science team helps solve research and development problems that are not easily answered by conventional analytical techniques. The Industrial Science team offers a range of rapid access programs for academic institutions and industry. Our scientists have a broad range of technical expertise, and we pride ourselves on quick responses to our clients and fast turn around times.

FULL SERVICE

Full Service offers quick and accurate solutions to industry questions. Our dedicated sector scientists develop an experimental outline based on the client's need and conduct all data collection and analysis. A detailed report provides all the key information for the client's question.

Because of CLS's expertise in tribology, chemical production giant BASF relies on the industrial science team to test their lubricant additives.

MX SERVICE

Macromolecular Crystallography (MX) is an essential technique for the study of proteins, nucleic acids and other large molecules that play key roles in pharmaceuticals and medical research. Our state of the art robotic systems and automated software make the CLS among the best MX facilities in the world. Remote access from anywhere in the world offers maximum flexibility for our clients.



ANALYTICAL SERVICE

PLANT PROFILING

Plant imaging options are customised for the needs of the customer, and cover project design, sample preparation, data collection, analysis and report writing. Plant profiling techniques include high-throughput bulk screening for elemental and organic components, bulk IR and IR mapping, μ CT and PCL. With this diverse range of techniques and service options, it is possible for us to offer a tailored and diverse solution package for characterizing and imaging a variety of plant tissues and environments based on the client's needs.

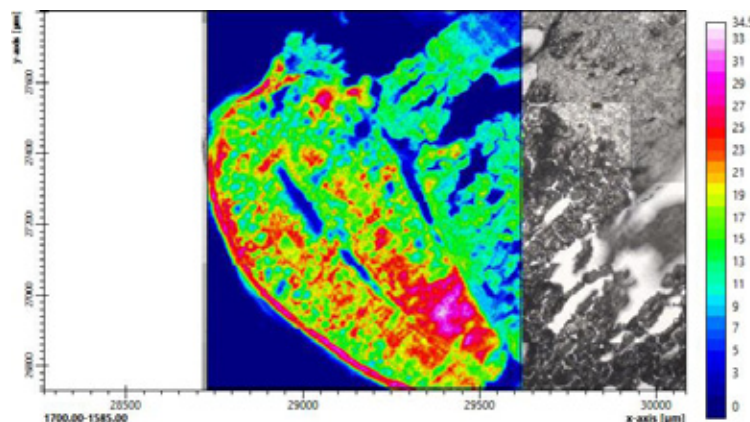
PXRD

Powder diffraction, or PXRD, is a versatile technique with applications in a wide variety of research sectors, from mineral exploration and environmental remediation, to pharmaceuticals and advanced functional materials. Our PXRD mail-in program provides researchers with affordable, rapid access to high quality data: the technique can be used to identify and quantify crystalline phases in complex mixtures, to solve and refine the crystal structures of important new materials and to examine microstructural features like crystallite size and strain.

SMALL MOLECULE

Small Molecule X-ray crystallography (SM-XRD) is an important analytical technique in material science, catalyst design as well as pharmaceutical and medical research. It is currently a key technique for directly determining the structure of small molecules and gaining insights into ligand-receptor interactions in biomedical research and substrate-catalysts interactions in catalysts design. It is also invaluable in the creation of new smart electronic materials and investigation of conformations of molecules and their packing.

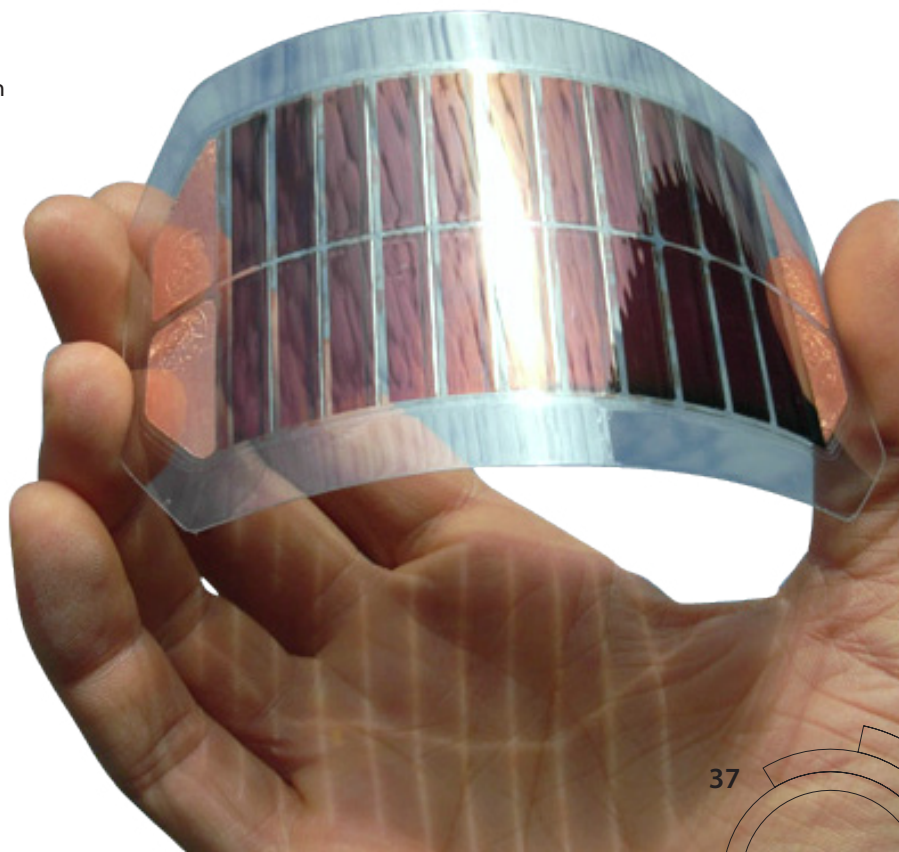
University of Alberta researchers are using CLS services to solve single crystal structures to help develop better organic solar cells.



Collaborations between the CLS and the University of Saskatchewan have shown the value in chemotyping various parts and pieces of plants.

PURCHASED ACCESS

CLS is one of the only facilities in North America to offer purchased access to beamtime for expert synchrotron users. This service does not require review by our external peer review committee, offering researchers rapid access to their desired beamlines. Researchers can also contact the Industrial Science group during April and October to request specific beamlines, techniques and dates for the next cycle.



EDUCATION PROGRAMS

Education programs at the CLS engage high school and undergraduate students in authentic research as a learning experience. Students, with mentorship from CLS staff and the user community, conduct curiosity-driven experiments with the potential to produce novel results.



Spruce it Up! Analysis of the Long Term Effects of Mining on Black Spruce Trees

Undergraduate work on IDEAS

Hudson Bay Mining and Smelting, Co. Limited began mining and smelting copper and zinc ores in the Flin Flon area in 1930 with continued smelting until 2010. Long-term effects of Hudson Bay's operations have included loss of vegetation in the surrounding boreal forest. Reforestation of the area has proven to be difficult due to metal contamination and soil acidification. Several remediation attempts through liming have been unsuccessful. Core samples of dead and living black spruce trees (*Picea mariana*) were collected at an affected site 16 km south of Flin Flon in 2014 as part of ongoing research into reforestation possibilities. Ring width was recorded, cross dated and standardized using WinDENDRO, COFECHA and ARSTAN at the University of Saskatchewan Mistik Askiwin Dendrochronology Laboratory (MAD Lab). Subsequently, XRF scans were performed on six samples at the IDEAS beamline. Dead trees within the smelter affected area showed higher concentrations of zinc and copper in the sapwood, the section of the tree trunk near the bark that transports nutrients, than in living trees.



Undergraduate students enrolled in Environmental Sciences 110 course participate in a First Year Research Experience, an initiative at the U of S. A subset of those students have the opportunity to collaborate with the MAD Lab and the CLS to conduct this research. Their work is presented in poster sessions.

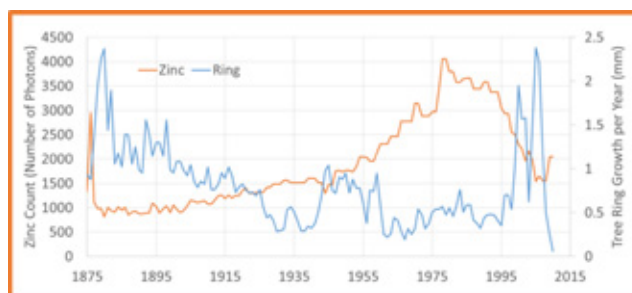


Figure 1: Ring growth and zinc concentration plotted against time shows -0.5 correlation.

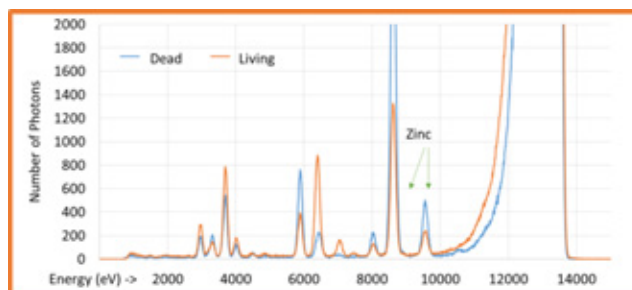


Figure 2: Dead trees showed higher levels of zinc than live trees.

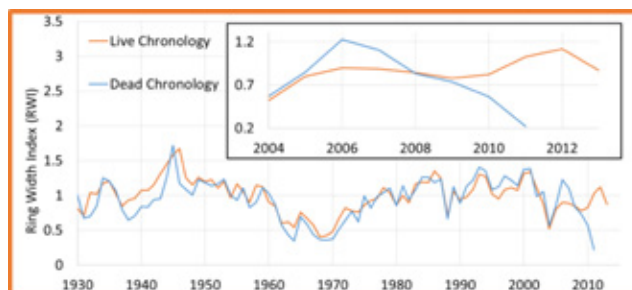
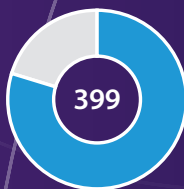


Figure 3: A standardized chronology comparison between a living and a dead population of black spruce. The highlighted portion and associated insert (black box) show the dieback year of the dead chronology which corresponds to higher levels of metals like zinc.

Beach, A.; Gelineau, J.; Jezowski, J.; Longworth, J.; Simonot, C.; Stark, B.; Nehemy, M. F.; Walker, T.; Laroque, C. P.

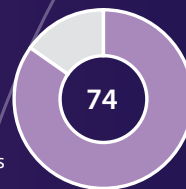
HANDS-ON CLS RESEARCH

- 339 high school students
- 60 post-secondary students



EDUCATORS ENGAGED WITH CLS

- 59 school teachers
- 15 post-secondary educators



NUMBER OF COMMUNITIES WITH STUDENTS AND/OR TEACHERS COMING TO CLS:

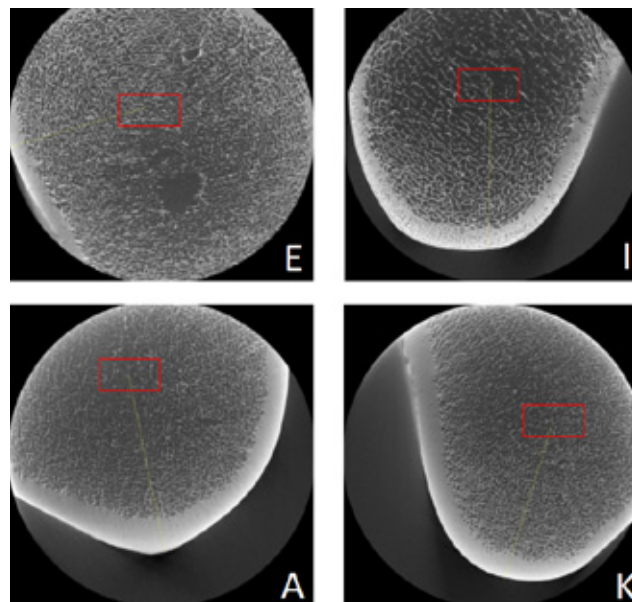
- 17 - SK
- 3 - AB
- 1 - QC
- 1 - NS
- 3 - ON
- 1 - MB

ENVIRONMENT

Polar bear express: Polychlorinated biphenyls and trabecular bone density of polar bear humerus bones

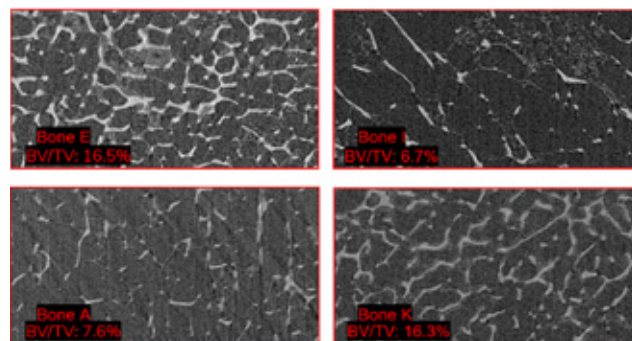
High school work on BMIT

Twelve high school students from Sundre High School in Sundre, Alberta investigated polychlorinated biphenyls (PCB) in relation to bone density in the trabecular area, the inner layer of the bone, of polar bear humerus bones. PCBs are manmade chemicals that were used in manufacturing household products since 1930's. With improper disposal, PCBs were first detected in the Canadian environment in 1966. By 1979 PCB use was banned in Canada. Many studies looked at bone density of polar bear bones, but very few looked within the trabecular area. Using the BMIT beamline, students compared the trabecular bone density of four humerus polar bear bones collected in 1960, 1967, 1971, and 2014. With the help of BoneJ, a data analysis tool, students looked at the volume fraction of the bone images collected. The volume fraction is the volume of mineralized bone per unit volume of the sample. Data suggests that there is a possible correlation between trabecular bone density and PCB exposure in polar bear humerus bones. Polar bears with lower PCB exposure had a higher trabecular bone density compared to polar bears with higher PCB exposure.



BMIT images of the four humerus polar bear bones. The red rectangle indicates the section that was analyzed using BoneJ to find the volume fraction.

- e) A 1960 adult bone with expected low PCB exposure;
- i) A 1971 juvenile bone with expected high PCB exposure;
- a) A 1967 adult bone with expected high PCB exposure;
- k) A 2014 adult bone with expected low PCB exposure.



BoneJ bone volume fraction (BV/TV) analysis of the trabecular area of four different polar bear humerus bones. Higher volume fractions indicate higher bone density, whereas lower volume fractions indicate lower bone density. Data suggests that Bone E and Bone K have higher bone density than Bone I and Bone K.

Beck, D., I. Brackley, D. Choi, D. Kamaledine, I. McElhinney, M. McElhinney, K. Mitchell-Chadwick, L. Sheridan, D. Valentine, B. Werdal, K. Wolfe, N. Wolfe, R. Beck, K. Challoner, L. Pankratz, M. A. Webb, N. Zhu A. Boechler.



Acronym Glossary

BEAMLINES

BioXAS: Biological X-ray Absorption Spectroscopy

BMIT: Biomedical Imaging and Therapy

BXDS: Brockhouse X-Ray Diffraction and Scattering Sector

CMCF: Canadian Macromolecular Crystallography Facility

CLS@APS: Canadian Light Source at Advanced Photon Source

Far-IR: Far Infrared Spectroscopy

HXMA: Hard X-ray MicroAnalysis

IDEAS: Industry Development Education Applications Students

Mid-IR: Mid Infrared Spectromicroscopy

REIXS: Resonant Elastic and Inelastic X-ray Scattering

SGM: High Resolution Spherical Grating Monochromator

SM: Soft X-ray Spectromicroscopy

SXRM: Soft X-ray Microcharacterization Beamline

SyLMAND: Synchrotron Laboratory for Micro And Nano Devices

VESPER: Very Sensitive Elemental and Structural Probe
Employing Radiation from a Synchrotron

VLS-PGM: Variable Line Spacing Plane Grating Monochromator

QMSC: Quantum Materials Spectroscopy Centre

TECHNIQUES

ABI: Analyzer-Based Imaging

CT: Computed Tomography

DEI: Diffraction-enhanced Imaging

EIS: Electrochemical Impedance Spectroscopy

EXAFS: Extended X-ray Absorption Fine Structure

IR: Infrared

FTIR: Fourier Transform Infrared Spectroscopy

MRT: Microbeam Radiation Therapy

PCI: Phase Contrast Imaging

RIXS: Resonant Inelastic X-ray Scattering

RXS: Resonant X-ray Scattering

SAXS: Small Angle X-ray Scattering

STXM: Scanning Transmission X-ray Microscopy

X-PEEM: X-ray Photoemission Electron Microscopy

XANES: X-ray Absorption Near Edge Structure

XAS: X-ray Absorption Spectroscopy

XES: X-ray Emission Spectroscopy

XPS: X-ray Photoelectron Spectroscopy

XRD: X-ray Diffraction

XRF: X-ray Fluorescence

THE BRIGHTEST LIGHT IN CANADA

2017






Canadian
Light
Source Centre canadien
de rayonnement
synchrotron

Canadian Light Source Inc.
44 Innovation Boulevard
Saskatoon, SK Canada S7N 2V3

Phone: (306) 657-3500
Fax: (306) 657-3535

www.lightsource.ca

 Canadian Light Source

 @canlightsource